NOAA Technical Memorandum OAR PMEL-125

PROCESSING OF SUBSURFACE ADCP DATA IN THE EQUATORIAL PACIFIC

P.E. Plimpton
H.P. Freitag
M.J. McPhaden

Pacific Marine Environmental Laboratory
Seattle, Washington
March 2004

NOTICE

Mention of a commercial company or product does not constitute an endorsement by NOAA/OAR. Use of information from this publication concerning proprietary products or the tests of such products for publicity or advertising purposes is not authorized.

Contribution No. 2635 from NOAA/Pacific Marine Environmental Laboratory

For sale by the National Technical Information Service, 5285 Port Royal Road
Springfield, VA 22161

Contents

List of Figures

List of Tables

Processing of Subsurface ADCP Data in the Equatorial Pacific

P.E. Plimpton, H.P. Freitag, and M.J. McPhaden

Abstract. Near-surface ocean currents are measured with acoustic Doppler current profilers (ADCPs) in the equatorial Pacific as part of the Tropical Ocean-Atmosphere/Triangle Trans-Ocean (TAO/TRITON) Array. Four equatorial sites at 110°W, 140°W, 170°W, and 165°E are presently maintained by the Pacific Marine Environmental Laboratory (PMEL) using upward-looking 153.6 kHz narrowband RD Instruments' ADCPs. The depths of the ADCP velocity data are determined to an accuracy of 5 m using historical sound velocity profiles and transducer depths computed by three independent methods. The measured ADCP velocities are corrected using sound velocities computed at the ADCP transducer from in situ temperatures and salinities. Data contaminated by sidelobe interference from sea surface reflections are eliminated and the ADCP velocities are mapped by interpolation to standard 5-m depths. ADCP velocities and directions are compared with velocity time series at specific depths collected on nearby surface moorings with EG&G mechanical current meters and with Sontek Argonaut-MD current meters. Mean velocity differences in these comparisons are less than 5 cm s^{-1} and mean direction differences are less than 5°.

1. Introduction

For more than two decades, upper-ocean and atmospheric variability has been monitored using an array of moored instruments in the tropical Pacific. These measurements provide long time series of upper-ocean temperatures, salinities, and currents, along with atmospheric parameters such as wind speed and direction, air temperature, and relative humidity, for analysis and monitoring of short-term climate variability and prediction of El Niño/Southern Oscillation (ENSO). Presently, approximately 70 moorings in the Tropical Atmosphere Ocean/Triangle Trans-Ocean Buoy Network (TAO/TRITON) Array (Fig. 1) provide measurements from 137°E to 95°W and 8°S to 8°N (McPhaden *et al.*, 2001). Prior to March 1999, EG&G Vector Averaging Current Meters (VACMs) and Vector Measuring Current Meters (VMCMs) were routinely used to measure equatorial currents at four or five specific depths at 110°W, 140°W, 156°E, and 165°E. With development of the Next Generation ATLAS mooring (Milburn *et al.*, 1996), these mechanical current meters (MCMs) were phased out and replaced with Sontek Argonaut-MD current meters. In early deployments of Argonaut-MDs at 110°W, 140°W, 170°W, and 165°E, the velocity measurements were biased low due to the instrument's inability to function properly in high current regimes (Freitag *et al.*, 2003). After instrument modification, high quality measurements of ocean currents at specific depths have been recorded for recent deployments with Argonaut-MDs mounted on equatorial taut-line moorings.

Beginning in 1988, currents in the upper equatorial Pacific Ocean have also been measured with RD Instruments' (RDI) 153.6 kHz acoustic Doppler current profilers (ADCPs). The first ADCP equatorial site was established with a subsurface mooring at 0°, 170°W, deployed by R. Weisberg (University of Florida at St. Petersburg). For approximately 5 years beginning in 1990 at 110°W and 1991 at 140°W, 156°E, and 165°E, equatorial ADCP velocities were also measured from PROTEUS (PROfile TElemetry of Upper

ocean currentS) surface moorings (McPhaden *et al.*, 1990). However, the accuracy of the surface-mounted ADCP measurements on the PROTEUS moorings was at times degraded due to the presence of pelagic fish which tend to school around equatorial moorings (Freitag *et al.*, 1992). ADCP velocity errors due to fish bias were corrected using coincident VACM and VMCM data (Plimpton *et al.*, 1995; 2000). No ADCP algorithms proved successful in removing the fish bias during data collection from surface deployments (Plimpton *et al.*, 1997), so the ADCPs were moved to separate subsurface moorings beginning in 1995. The subsurface ADCP data did not exhibit the increase in echo amplitude and decrease in velocity magnitude associated with the acoustic reflections from pelagic fish that were evident in the surface moored ADCPs.

By January 1996, all equatorial ADCPs were mounted on separate subsurface moorings. The Japan Marine Science and Technology Center (JAMSTEC) deployed the subsurface ADCPs at 0°, 165°E from 1997 to 2001 and also established a subsurface ADCP site at 0°, 147°E in 1994. Presently, the Pacific Marine Environmental Laboratory (PMEL) maintains subsurface ADCP deployments on the equator at 110°W, 140°W, 170°W, and 165°E. This report describes the techniques used at PMEL to process the subsurface ADCP data from the equatorial Pacific and compares the ADCP measurements with VACM/VMCM and Argonaut-MD velocities measured on nearby moorings.

2. Instrumentation

The RDI ADCP is a four-beam system that transmits a high-frequency acoustic pulse, measures the Doppler shift in the backscattered acoustic energy as a function of time, and computes the beam-direction velocity component as a function of range (Gordon, 1996). Using compass measurements, the range-gated ADCP beam velocities are then converted into vertical profiles of zonal and meridional velocity. The ADCP compass (manufactured by KVH Industries, Inc., Middletown, Rhode Island) is calibrated at PMEL to an accuracy of ±2.5 degrees.

The frequency shift measured by the ADCP is caused by the relative motion of scatterers, generally plankton, whose movement is assumed to be due, on the average, to oceanic advection. However, scatterers have been found to swim against or at least non-coincident with the main current flow, resulting in horizontal velocity measurement errors up to 30 cm s^{-1} (Wilson and Firing, 1992; Moore and Stewart, 2003). The amount of error in the reflected pulse due to reflections from coherent horizontal swimmers is dependent on the reflective characteristics of specific species associated with the acoustic frequency of the ADCP and the variable species concentrations at different depths which changes with diurnal migration. Velocity errors due to reflections from horizontal swimmers are not obvious when data from TAO upward-looking equatorial subsurface ADCPs are compared with VACM/VMCM or Argonaut-MD velocities.

TAO subsurface ADCP moorings are generally recovered and redeployed

Table 1: PMEL equatorial mooring deployments for subsurface ADCPs.

	Start time/date					End time/date				
110°W:										
EA01	0	00	12	8	95	23	00	18	5	96
EA02	6	00	19	5	96	14	00	9	10	96
EA02b	3	00	10	10	96	1	00	22	2	97
EA03	23	00	23	2	97	23	00	27	2	98
EA04	7	00	1	3	98	14	00	10	5	99
EA05	21	00	10	5	99	20	00	14	11	99
EA06	6	00	15	11	99	2	00	8	5	00
EA07	19	00	8	5	00	12	00	7	4	01
EA08	22	00	8	4	01	20	00	11	3	02
140°W:										
CA01	lost									
CA02	1	00	4	9	96	1	00	21	10	97
CA03	8	00	21	10	97	23	00	27	9	98
CA04	10	00	28	9	98	16	00	19	9	99
CA05	0	00	21	9	99	18	00	22	9	00
CA06	3	00	23	9	00	16	00	9	9	01
CA07	2	00	10	9	01	18	00	26	8	02
170°W:										
KA01	2	00	28	7	96	17	00	23	5	97
KA02	3	00	24	5	97	1	00	23	6	98
KA03	11	00	23	6	98	23	00	18	7	99
KA04a	12	00	20	7	99	0	00	5	11	99
KA04b	10	00	5	11	99	6	00	2	7	00
KA05	5	00	4	7	00	17	00	17	6	01
KA06	3	00	18	6	01	23	00	19	6	02
165°E:										
WA01	5	00	29	1	96	23	00	10	7	96
WA01b	12	00	11	7	96	20	00	30	1	97
WA01c	8	00	31	1	97	6	00	13	6	97
WA02a	1	00	6	4	01	1	00	9	7	01
WA02	8	00	9	7	01	18	00	3	11	01

once a year (Table 1). The 153.6 kHz narrowband RDI ADCPs have a 20 degree transducer orientation and are set to collect data with 8.68 m nominal bin and pulse lengths. The ADCP measurements represent a weighted-average over two bin widths, available for every single bin width interval. The instruments collect data at a 3-second sample rate and form averages over 15 minutes beginning at the top of the hour. The theoretical random error in horizontal current speed, determined by the ADCP frequency, the bin and pulse widths, and the number of pings averaged, is less than 1 cm s^{-1}. The ADCPs at 110°W, 140°W, and 165°E are set to use a broad low pass filter bandwidth (600 Hz) to minimize skew error in the high shear regimes (Pullen *et al.*, 1992). The 170°W ADCP is set to use a narrow low pass filter bandwidth (300 Hz) to maintain the original settings begun in 1988 and because of lower shear in the 170°W velocity measurements. The upward looking transducers are deployed at nominal depths of 250 to 300 m

below the sea surface. The data are recorded in the instrument's memory and retrieved after mooring recovery.

Two pressure sensors are mounted 2 meters below the ADCP transducer. A model 16 Seacat or 37-SM MicroCAT, both manufactured by Sea-Bird Electronics (SBE) of Bellevue, Washington, is paired with either a minitemperature pressure recorder (MTPR) or a Next Generation Atlas temperature pressure (TP) recorder, manufactured at PMEL. The pressure sensors in the Seacat, the MTPR and the TP were developed by Paine Corporation of Seattle, Washington, with a range of 0 to 690 m and an accuracy of 0.25% of full range or 1.7 m. The MicroCAT pressure sensor, developed by Druck, Inc. of New Fairfield, Connecticut, has a range of 0 to 1000 m with an accuracy of 0.1% of full range or 1 m. For the 27 subsurface deployments listed in Table 1, 19 deployments had pressure data from both sensors for all or most of the deployment. For these deployments, the depth determined from the SBE sensor generally agreed to within 1 m with the depth determined from the PMEL sensor. The average depth difference for any instrument pair did not exceed 2.6 m for any deployment.

3. Transducer Depth

The ADCP mooring line is measured so that the transducer's shallowest depth (with the mooring line fully extended vertically) is between 250 m and 300 m. However, this deployment depth can vary between deployments due to different ocean depths at the actual deployment site and replacement of the mooring line components (Fig. 2). In addition, the actual depth of the ADCP transducer head is variable in time, as the PMEL subsurface mooring reacts to variations in ocean currents beneath the instrument. The greatest changes in transducer depth have occurred at 0°, 170°W, where the difference between the minimum and maximum transducer depth exceeded 200 m for the KA03 deployment (Fig. 2c). Transducer depth excursions for three of the six deployments at 0°, 140°W exceeded 100 m (Fig. 2b). At 0°, 110°W, the depth excursions were generally smaller and did not exceed 80 m for any deployment except for the EA01 deployment (Fig. 2a). The smallest head depth variability occurred at 0°, 165°E, where only one deployment experienced excursions as large as 75 m (Fig. 2d). Initial subsurface ADCP moorings were deployed using a 3/8″ diameter double-braided Kevlar polyester construction. Large depth excursions of the mooring flotation ball (as described above) were not coherent with currents measured above the ball. Thus the excursions were attributed to drag on the mooring line at greater depths and an alternate line with reduced drag characteristics was sought. On moorings deployed in 2000 and after, the majority of line used (at minimum the line for the upper 2000 m of the mooring) was a custom PMEL product of 1/4″ diameter and polyethylene jacketed Vectran construction. Moorings deployed with this line have shown a decrease in depth excursions of the subsurface flotation (Fig. 2).

Because of the variation in the depth of the ADCP transducer during a deployment, accurate determination of the transducer depth is critical for

correct depth mapping of the velocity measurements. Upon recovery, the SBE pressure sensor is compared with the PMEL sensor to verify agreement to within instrument accuracies. If both sensors function properly for the duration of the deployment, the SBE pressure values are used to determine the transducer depth. Pressure is converted to depth using gravity adjusted for latitude and depth, along with density profiles averaged for each deployment site from historical conductivity/temperature/depth (CTD) data.

An independent estimate of the transducer depth is also determined from the ADCP echo amplitude data and compared with the depth derived from the pressure sensors. For each hourly profile, the water mass volume backscatter strength (target strength) for each beam and each depth bin is computed from the echo amplitudes (Appendix 1). The PMEL ADCPs are not calibrated for determination of an absolute target strength, but rather a relative target strength profile is calculated. This calculation adjusts the echo amplitudes for the effects of beam spreading and signal absorption and results in a target strength profile where the surface reflection appears as a maximum (Fig. 3). A second-order polynomial is fit in depth to the three largest target strengths for each beam. To determine the strength of the surface reflection, the mid-depth ($\sim$150 m) target strength is subtracted from the maximum target strength determined from the polynomial fit. If the target strength difference is too low (generally less than 40 dB) for any beam, the target strength is not used to determine a transducer depth for the hourly profile. Less than 10% of the hourly profiles have surface reflection signals too small to compute the transducer depth.

The bin numbers of the three bins closest to the surface are then used to compute the nominal distance between each echo amplitude bin and the transducer using

$$\text{distance} = \text{blnk} + \text{abs}(\text{P} - \text{BW})/2 + (\text{N} * \text{BW}) + (\text{BW}/4) \qquad (1)$$

where for a system with transducers set at 20 degrees from vertical

blnk	=	4.34 m, the nominal blanking
P	=	8.68 m, the nominal pulse length
BW	=	8.68 m, the nominal bin width
N	=	bin number

The BW/4 factor is included because the ADCP samples the echo amplitude in the last quarter of each depth cell. The polynomial fit to the three bins is then used to compute the nominal distance of the maximum target strength from the transducer. This distance is computed for each of the four beams and averaged. The average nominal distance of the surface with respect to the transducer is used as the nominal depth of the instrument for each hourly profile.

The nominal depth assumes a constant sound speed with depth of 1475.1 m s^{-1}. Mean historical sound velocity profiles, computed for each site from historical CTD data, are used to convert the nominal depth to the actual

transducer depth.

$$\text{actual depth} = \text{nominal depth} * \text{C}/1475.1 \text{ m s}^{-1} \quad (2)$$

where C is the mean sound velocity for a given depth interval. For PMEL processing, the sound speed adjustment was made for each 1 meter of depth and interpolated over the depth of the transducer for each hourly ensemble. At 500 m, the actual depth is deeper than the nominal depth by ∼10 m in the eastern Pacific and ∼13 m in the western Pacific. The uncertainty in computing the actual depth from the nominal depth with historical CTD data is ±2 m, determined by using historical sound speeds ±2 standard deviations over the 500 m depth range.

Comparison of the transducer depth determined from target strength and from the pressure sensors was performed for all but the earliest deployments. Deployment mean differences were usually within ±3 m and did not exceed 6.5 m, which is approximately two-thirds of the actual ADCP bin width. The differences arise from errors in the pressure sensor measurement which has a 1.7 m accuracy (Sea-Bird Electronics, 1996), the computation of actual depth using historical sound speeds which has a 2 m accuracy (Plimpton *et al.*, 1995), and the precision of determining the location of the surface by a second-order polynomial fit to three ADCP depth bins which are generally 9 m apart near the sea surface.

For deployment EA03 at 0°, 110°W, both pressure sensors failed by 14 September 1997 during the yearlong deployment beginning in February 1997. Comparison of the transducer depth determined from the Seacat pressure versus target strength for the first $6\frac{1}{2}$ months of the deployment indicate excellent agreement, with a mean difference of 0.16 m and difference rms of 0.55 m (Fig. 4). Thus, the target strength calculation was used for the transducer depth for the remaining $5\frac{1}{2}$ months of the deployment. A transducer depth was computed from the target strength for 96% of the hourly ADCP profiles during this period. Interpolation between the computed transducer depths was used to fill the 4% of data for which the transducer depth could not be computed due to a minimal surface reflection signal.

4. Data Processing

For subsurface ADCPs, the depth of the center of the first velocity bin (closest to the transducer) is determined by the transducer depth (typically computed from the SBE instrument) and the velocity of sound at that depth. The nominal distance of the first velocity bin from the transducer is computed using

$$\text{distance} = \text{blnk} + \text{abs}(\text{P} - \text{BW})/2 + (\text{N} * \text{BW}) \quad (3)$$

where for a system with transducers set at 20 degrees from vertical

blnk	=	4.34 m, the nominal blanking
P	=	8.68 m, the nominal pulse length
BW	=	8.68 m, the nominal bin width
N	=	bin number

The nominal distance is converted to an actual distance using (2). The actual distance is then subtracted from the transducer depth to compute the bin 1 depth. As stated above, the sound velocity for a given depth is determined from an averaged historical sound speed profile for each mooring site. As the transducer changes depth during the deployment, a different portion of the sound speed profile is used for the mean sound speed for each bin. After the actual distance of each bin from the transducer is computed from the nominal distance, it is subtracted from the transducer depth to get the depth of each velocity bin for each hourly profile. Since the depths of the center of the ADCP bins vary for each hourly profile, the velocity data are mapped by interpolation to standard 5-m depths.

Prior to interpolation of the ADCP velocities to standard depths, several corrections are made to the data:

The ADCP velocity measurements assume a constant sound speed of 1536 m s^{-1} at the transducer. Temperature and salinity data from the SBE Seacat or MicroCAT, mounted 2 m below the transducer, are used to compute hourly sound speeds and correct the velocities by the equation:

$$\text{corrected velocity} = \text{measured velocity} * \text{sound speed}/1536 \text{ m s}^{-1} \quad (4)$$

The near surface velocity measurements may be in error due to strong reflections from the surface that overcome the sidelobe suppression of the transducer. Hourly data are flagged bad if the bin depth (the center of the velocity bin) is closer to the surface than

$$D' = D * (1 - \cos(\theta)) + \text{bin width} \quad (5)$$

where D' is the depth below which sidelobe interference is not a problem, D is the transducer depth, θ is the angle of the transducer beam relative to vertical, and the bin width has been adjusted for sound velocity. Since the ADCP measurement is a weighted average over a two-bin width range, half the range (1 bin width) must be added to the depth of the sidelobe interference (as shown in (5) to avoid error in the ADCP measurement. For an hourly transducer depth of 300 m and an instrument beam angle of 20 degrees, D*(1-cos(θ)) equals 18.09 m. At 110°W, the historical sound speed at 18 m is 1530.5 m s^{-1}. The 8.68 m nominal bin width is adjusted for sound velocity using (2). The adjusted bin width, equal to 9.01 m, plus 18.09 m, gives a sidelobe interference cutoff depth of 27.1 m. Thus the velocity data for this example would be set bad for all depth bins centered at a depth shallower than 27.1 m.

Finally, the ADCP bin depths are adjusted for a deployment if the mean difference between the transducer depth computed from the pressure sensor and the depth computed from the target strength exceeds 5 m. This adjustment is made to ensure a 5-m accuracy in the depth of the ADCP velocity measurements. The difference between the computed depths is used to maximize the depth accuracy of all bins in the profile. Near the transducer, the depth error should not exceed the 1.7 m expected accuracy of the pressure sensor. As the distance from the transducer increases, the depth error may increase due to the use of a historical sound speed profile for

conversion of the nominal bin widths, resulting in a maximum error at the sea surface. Conversely, the target strength from the surface reflection can be used to determine the bin depths without error due to the pressure sensor measurements. Bin depths based on the surface reflection would have sound speed depth errors which increase with depth, resulting in minimal depth error near the surface and maximum depth error near the transducer. To minimize depth error in the profiles originally referenced to the pressure sensor, the computed target strength/pressure sensor difference is applied incrementally over the profile to adjust the bin depths from the transducer to the surface. This integrated adjustment is applied such that no adjustment is made at the transducer and the maximum adjustment is made at the surface. Depths have been adjusted for 5 of the 27 deployments (less than 20%), with adjustment values ranging from 5 to 6.5 m.

5. Instrument Comparisons

The ADCP velocities and current directions are routinely compared with coincident point velocity measurements when available on nearby (generally within 5–15 km) surface moorings. Velocities measured with the subsurface ADCP are compared with mechanical current meter (MCM) velocities for all coincident equatorial deployments at 45 m, 80 m, and 120 m at 110°W and 140°W and at 50 m, 100 m, and 200 m at 165°E. MCM data were also collected at all three sites at 10 m, along with 25 m data at 110°W and 140°W. Due to sidelobe interference from surface reflections, the shallowest ADCP velocity values, coincident with the MCM data, were at 30 m at 140°W and 165°E. At 110°W, only 16% of the hourly data had values at 25 m. Thus, no comparisons were made at the 10 m and 25 m depths. The MCMs were replaced with Sontek Argonaut-MDs on equatorial surface moorings in 1998 at 110°W and in 1999 at 140°W and 165°E. Point velocity measurements with Argonaut-MDs began in 2000 at 0°, 170°W. At the time of this report, data are only available for ADCP comparison with Argonaut-MDs at 0°, 110°W and 0°, 140°W.

The MCMs were either EG&G Vector Averaging Current Meters (VACMs) or Vector Measuring Current Meters (VMCMs). Tow tank runs performed on VACMs by PMEL indicate that the rotor is accurate to within 1.2 cm s^{-1} in steady flow. While the absolute accuracy of a surface-moored VACM is unknown, there is evidence that it slightly overestimates current velocity in highly variable flows (Beardsley, 1987; Karweit, 1974). On the other hand, the VACM has been found to slightly underestimate velocity by a few percent in highly variable reversing flows (Weller and Davis, 1980). The VMCMs use a flux gate compass, similar to the one used in the ADCP, calibrated to an accuracy of ±2.5°. During pre-deployment checkout, the VACM mechanical compass linearity (compass error relative to a chosen fixed direction) was confirmed to be ±5.6° or less, but absolute accuracy is undetermined.

At 0°, 110°W, the ADCP subsurface measurements began in August of 1995, but the nearby surface mooring for that deployment was lost. Thus, ADCP and MCM measurements are compared for all available deployments

between May 1996 and February 1998, when the last 110°W MCMs were recovered. At times, an MCM for a given deployment at a specific depth would fail or collect measurements with obvious errors in velocity magnitude or direction. The data from these MCMs are not included in the comparison with the ADCP data. Thus, the number of comparison days at given MCM depths will differ.

Figures 5–7 show scatter plots comparing the 110°W MCM and ADCP velocity and direction measurements at 45 m, 80 m, and 120 m, respectively. Statistical results of the 0°, 110°W MCM and ADCP comparisons of daily averaged zonal velocity, meridional velocity, speed, and direction are given in Table 2. For the periods of coincident data, the ADCP mean, the ADCP standard deviation, the ADCP minus MCM mean difference, and the difference root mean square (rms) are listed. The maximum mean velocity difference, 2.1 cm s^{-1}, occurs in the meridional velocity comparison at 120 m. The rms of the velocity differences do not exceed 6.0 cm s^{-1}. Current directions agree to within 2.1° for all three depths, with a maximum rms of the direction differences equal to 10.4°.

At 0°, 140°W, the ADCP subsurface measurements began in September of 1996, allowing comparison with MCMs through final MCM recovery in February 1999. The good agreement in velocity and direction measurements during this $2\frac{1}{2}$ year time period is shown in Figs. 8–10 for 45 m, 80 m, and 120 m, respectively. The statistics of this comparison are listed in Table 2. At 0°, 140°W, mean velocity differences do not exceed 4.1 cm $s^{-1,}$ with the rms of the differences less than 7 cm s^{-1}. Mean directions at 0°, 140°W agree to within 3.4° and the maximum rms of the direction differences is 11.4°. The number of days of data comparison varies with depth due to periodic MCM failure.

At 0°, 165°E, the ADCP velocities are compared with MCM velocities measured at 50 m, 100 m, and 200 m. PMEL subsurface ADCP velocity measurements, coincident with MCM measurements, were collected at 0°, 165°E between January 1996 and June 1997. Figures 11–13 show scatter plots comparing the 165°E ADCP and MCM velocity and direction measurements at 50 m, 100 m, and 200 m, respectively. The statistics of the ADCP and MCM comparison at these three depths are listed in Table 2. The maximum mean differences occur at 100 m for speed, –2.8 cm s^{-1}, and direction, –2.0°. The maximum difference rms for velocity is 6.1 cm s^{-1} and for direction is 13.4°. The number of comparison days varies with depth due to periodic MCM failure.

Beginning in 1996, PMEL began deployments of the Next Generation ATLAS mooring (Milburn *et al.*, 1996), with inductive data telemetry using the main subsurface mooring cable. The MCMs could not easily be inserted into the conducting mooring cable used with this mooring design. Also, the MCMs were difficult to maintain due to obsolete mechanical and electronic parts. Thus, beginning in 1998, the MCMs were replaced with Sontek Argonaut-MD current meters.

The Sontek Argonaut-MDs, which are clamped to the mooring cable, have three transducers oriented 45° from the instrument's vertical axis. The transducers transmit a 0.5-m long acoustic pulse and measure the Doppler

Table 2: Statistics are shown for the comparison of daily averaged ADCP data collected on the equator at 110°W, 140°W, and 165°E with MCMs mounted on nearby surface moorings. For the periods of coincident data, the ADCP mean, the ADCP standard deviation, the ADCP minus MCM mean difference, and the difference root mean square are listed for zonal velocity, meridional velocity, speed, and direction.

	zonal velocity				meridional velocity				speed				direction				daily values
	mean cm/s	stan dev cm/s	mean diff cm/s	diff rms cm/s	mean cm/s	stan dev cm/s	mean diff cm/s	diff rms cm/s	mean cm/s	stan dev cm/s	mean diff cm/s	diff rms cm/s	mean deg	stan dev deg	mean diff deg	diff rms deg	
ADCP and MCM Comparison at 0°, 110°W May 1996 to February 1998																	
45 m	32.2	37.8	**− 0.7**	4.4	−3.7	24.5	**−0.4**	3.5	47.1	29.4	**−1.3**	4.1	127.9	76.3	**−0.6**	10.4	466
80 m	78.5	38.0	**1.8**	5.7	5.7	17.2	**0.0**	5.0	81.1	36.8	**1.7**	5.8	87.2	29.3	**0.0**	6.0	476
120 m	62.1	17.0	**1.5**	3.2	2.3	12.3	**−2.1**	3.2	63.5	16.6	**1.4**	3.1	88.5	12.8	**2.1**	3.1	141
ADCP and MCM Comparison at 0°, 140°W September 1996 to February 1999																	
45 m	27.0	44.9	**4.1**	6.2	−3.9	28.4	**−1.9**	6.1	62.3	39.4	**0.3**	5.7	139.1	84.0	**2.1**	11.4	504
80 m	71.6	39.3	**1.3**	4.6	−0.5	23.2	**−0.8**	5.1	78.2	33.8	**1.4**	4.6	101.6	45.3	**1.1**	7.0	330
120 m	57.3	45.1	**1.1**	5.4	−2.3	15.1	**−3.7**	6.8	66.5	33.5	**1.0**	4.9	115.3	64.3	**3.4**	11.1	531
ADCP and MCM Comparison at 0°, 165°E January 1996 to June 1997																	
50 m	−15.2	29.3	**0.5**	5.2	0.0	10.6	**−2.4**	6.1	30.5	16.7	**−1.2**	5.3	222.5	85.2	**−1.6**	11.8	238
100 m	12.7	25.9	**−1.4**	4.1	0.6	12.9	**−0.6**	3.4	27.8	15.0	**−2.8**	4.3	149.3	95.6	**−2.0**	13.4	338
200 m	45.7	15.5	**0.4**	4.0	−0.5	9.0	**−1.2**	4.8	46.8	14.8	**0.3**	4.0	89.5	15.6	**1.1**	7.3	371

Table 3: Statistics are shown for the comparison of daily averaged ADCP data collected at 0°, 110°W and 0°, 140°W with sontek Argonaut-MDs mounted on nearby surface moorings. For the periods of coincident data, the ADCP mean and standard deviation, the ADCP minus Argonaut-MD mean difference, and the difference root mean square are listed for zonal velocity, meridional velocity, speed, and direction.

	zonal velocity				meridional velocity				speed				direction				daily values
	mean cm/s	stan dev cm/s	mean diff cm/s	diff rms cm/s	mean cm/s	stan dev cm/s	mean diff cm/s	diff rms cm/s	mean cm/s	stan dev cm/s	mean diff cm/s	diff rms cm/s	mean deg	stan dev deg	mean diff deg	diff rms deg	
ADCP and Argonaut-MD Comparison at 0°, 110°W April 2001 to September 2001																	
45m	97.4	68.8	**−1.5**	6.6	−5.9	26.2	**3.9**	5.5	107.4	58.3	**−3.6**	6.2	114.6	57.3	**−3.2**	6.5	159
120m	59.1	21.0	**4.3**	4.9	−2.5	14.4	**0.7**	2.3	61.1	20.4	**4.5**	5.0	93.0	15.9	**−1.1**	2.6	165
ADCP and Argonaut-MD Comparison at 0°, 140°W September 2001 to August 2002																	
25m	6.1	45.8	**0.3**	3.6	1.2	23.2	**0.4**	3.0	44.0	27.2	**0.1**	3.5	157.9	96.6	**−0.5**	10.6	295
45m	26.5	46.5	**2.3**	4.7	−0.1	21.8	**−0.5**	3.3	50.8	27.6	**2.7**	4.5	128.6	78.2	**−1.4**	8.2	270
80m	76.6	50.6	**3.3**	4.9	−3.2	17.7	**2.6**	4.8	83.8	41.6	**2.4**	4.4	103.4	43.1	**−3.0**	6.4	251

shift in the backscattered acoustic energy from a range set to be 0.5 m to 2.0 m vertically from the instrument. The beam-direction velocities, computed from the measured Doppler shift for each beam, are converted to earth coordinates using the relative transducer orientation and a Precision Navigation compass. The Argonaut-MDs were generally set to collect data once per second for 180 seconds at a 600-second interval. The theoretical accuracy of the Argonaut-MD velocity measurement is 1.8 cm s^{-1} and the compass is 2.0°. Early tests by PMEL indicated that the Argonaut-MD measurements compared well with coincident ADCP velocities, but later comparisons revealed that the Argonaut-MD horizontal current speed was biased low (Freitag *et al.*, 2003). Investigation revealed that the bias was due to the inability of the Argonaut-MD compass/tilt-sensor (Precision Navigation model TCM2) to function properly on moorings deployed in high current regimes where the instruments experience extreme lateral and rotational accelerations. Beginning in 2001, PMEL began to attach vanes to each instrument to reduce the acceleration of the current meters on the mooring lines. Subsequently, differences between ADCP and Argonaut-MD measurements have been comparable to those found between ADCP and MCM measurements.

Vanes were attached to the Argonaut-MDs at 0°, 110°W beginning in April 2001 for 7 months, coincident with a nearby, yearlong ADCP deployment. The next deployment of Argonaut-MDs at 0°, 110°W was also coincident with the ADCP deployment, but the Atlas surface mooring was pulled upon several times by fishing vessels. Within a month of deployment, the mooring had been moved from its original location by 23 km and then moved an additional 22 km by the end of the second month. Thus, data from the second 0°, 110°W deployment are not included in the ADCP/Argonaut-MD comparisons. For the first deployment (April 2001) Argonaut-MD measurements were collected at 10 m, 25 m, 45 m, 80 m, and 120 m, but the alkaline batteries failed after 4 months at 25 m and after 5 months at 10 m and 45 m. In addition, velocities and directions at 25 m and 80 m were flagged as bad due to low acoustic signal intensities for the whole deployment. Measurements at 120 m were also flagged as bad after 25 September 2001 due to a drop in instrument signal intensity. Scatter plots of the remaining 45 m and 120 m measurements are shown in Figs. 14 and 15. No ADCP data is available at 10 m due to sidelobe interference from reflections from the sea surface. Statistics for the 45 m and 120 m measurement comparisons are shown in Table 3. Mean velocity differences do not exceed 4.5 cm s^{-1} and mean direction differences do not exceed 3.2°. The maximum difference rms is 6.6 cm s^{-1} for velocity and 6.5° for direction. The number of days of data comparison varies due to Argonaut-MD battery failure and insufficient signal strength.

At 0°, 140°W, two deployments of Argonaut-MDs with attached vanes are coincident with ADCP measurements available as of this time. The first was from 11 September 2001 to 4 May 2002, and the second from 6 May 2002 to 27 August 2002. Argonaut-MDs were located on the taut-line moorings at 5 depths, 10 m, 25 m, 45 m, 80 m, and 120 m. For both deployments, the 120 m depth Argonaut-MDs did not function properly due to low acoustic signal intensities. Alkaline batteries, which lasted only $4\frac{1}{2}$ to 6 months at the

various depths, were used to power the Argonaut-MDs for the 8-month-long first deployment. Beginning with the May 2002 deployment, the alkaline batteries have been replaced with lithium batteries.

The shallowest good hourly ADCP velocity values at 0°, 140°W from September 2001 to August 2002 range from 26 m to 35 m after rejection of the near surface data due to sidelobe interference. To allow comparison with the 25 m Argonaut-MD data at this location, the hourly ADCP velocities were linearly extrapolated to 25 m, using the shallowest two good ADCP velocities before mapping to standard 5-m depths. Scatter plot comparisons of the ADCP data with the Argonaut-MD measurements are shown at 25 m, 45 m, and 80 m (Figs. 16–18). Statistics for these comparisons are listed in Table 3. At 0°, 140°W, ADCP minus Argonaut-MD mean velocity differences do not exceed 3.3 cm s^{-1} and mean direction differences do not exceed 3.0°. The maximum difference rms is 4.9 cm s^{-1} for velocity and 10.6° for direction. The number of comparison days varies due to the time of Argonaut-MD battery failure at each depth for the first deployment.

6. Summary

Subsurface ADCP data provide hourly profiles of zonal and meridional velocity as part of the TAO/TRITON array of tropical Pacific moorings. The ADCP transducer is deployed at a nominal depth of 250 to 300 m, but the depth of the transducer can vary as much as 200 m during a deployment due to drag on the mooring line from ocean currents beneath the instrument. The depth of the instrument is computed to a 5-m depth accuracy from pressure time series recorded by duplicate sensors mounted near the ADCP transducers and by the reflection of the sea surface evident in the ADCP echo amplitude. The ADCP velocities and nominal bin widths are adjusted for sound velocity. The near surface velocities contaminated by sidelobe interference from sea surface reflections are set bad. The remaining velocities are mapped by interpolation to standard 5-m depths and compared with coincident point velocity measurements, from EG&G mechanical current meters or Sontek Argonaut-MD current meters, regularly available on nearby surface moorings. Mean velocity differences in these comparisons are less than 5 cm s^{-1} and mean direction differences are less than 5°.

The zonal and meridional velocities collected on subsurface ADCP moorings are included in the TAO ADCP database. Contour plots of the PMEL subsurface data are shown in Figs. 19–22 for the equatorial sites at 110°W, 140°W, 170°W, and 165°E, respectively. The velocities shown at 165°E include data provided by JAMSTEC. ADCP velocities continue to be collected at these sites; however, processed velocities from the 2002–2003 deployments are not yet available. These data are part of the tropical Pacific ocean/atmosphere archive maintained by PMEL from deployments supported by PMEL and JAMSTEC. Data are publicly available at `www.pmel.noaa.gov/tao/data-deliv/`.

7. Acknowledgments

This work was supported by NOAA's offices of Global Programs and Oceanic and Atmospheric Research. The authors are grateful to Dave Zimmerman who provided the expert engineering work required for the deployment, recovery, and maintenance of the Argonaut and ADCP instruments.

References

Beardsley, R.C. (1987): A comparison of the vector-averaging current meter and New Edgerton, Germeshausen, and Grier, Inc., vector-measuring current meter on a surface mooring in Coastal Dynamics Experiment 1. *J. Geophys. Res.*, *92*, 1845–1859.

Flagg, C.N., and S.L. Smith (1989): On the use of the acoustic Doppler current profiler to measure zooplankton abundance. *Deep-Sea Res.*, *36*, 455–474.

Francois, R.E., and G.R. Garrison (1982): Sound absorption based on ocean measurements. Part II: Boric acid contribution and equation for total absorption. *J. Acoust. Soc. Am.*, *72*(6), 1879–1890.

Freitag, H.P., M.J. McPhaden, C. Meinig, and P.E. Plimpton (2003): Mooring motion bias of point-doppler current meter measurements. In *Proceedings of the IEES/OES Seventh Working Conference on Current Measurement Technology*, San Diego, CA, 13–15 March 2003, 155–160.

Freitag, H.P., M.J. McPhaden, and P.E. Pullen (1992): Fish-induced bias in acoustic Doppler current profiler data. In *Oceans '92, Mastering the Oceans Through Technology*, Newport, RI, 26–29 October 1992, 712–717.

Gordon, R.L. (1996): Acoustic Doppler current profilers, principles of operation: A practical primer. R.D. Instruments, 51 pp. [Available from R.D. Instruments, 9855 Businesspark Ave., San Diego, CA 92131].

Karweit, M. (1974): Response of a Savonious rotor to unsteady flow. *J. Mar. Res.*, *32*, 359–364.

McPhaden, M.J., T. Delecroix, K. Hanawa, Y. Kuroda, G. Meyers, J. Picaut, and M. Swenson (2001): The El Niño/Southern Oscillation (ENSO) Observing System. Observing the Ocean in the 21st Century, Australian Bureau of Meteorology, Melbourne, Australia, 231–246.

McPhaden, M.J., H.B. Milburn, A.I. Nakamura, and A.J. Shepherd (1990): PROTEUS—Profile telemetry of upper ocean currents. In *Proceedings of the MTS '90 Conference*, Marine Technology Society, Washington, D.C., 26–28 September, 353–357.

Milburn, H.B., P.D. McLain, and C. Meinig (1996): ATLAS Buoy—Reengineered for the next decade. In *Proceedings of the Oceans 96 MTS/IEEE Conference*, Fort Lauderdale, FL, 23–26 September 1996, 698–702.

Moore, A.N., and D.L. Stewart (2003): The effects of mobile scatterers on the quality of ADCP data in differing marine environments. In *Proceedings of the IEES/OES Seventh Working Conference on Current Measurement Technology*, San Diego, CA, 13–15 March 2003, 202–206.

Plimpton, P.E., H.P. Freitag, and M.J. McPhaden (1995): Correcting moored ADCP data for fish-bias errors at 0°, 110°W and 0°, 140°W from 1990 to 1993. NOAA Tech. Memo. ERL PMEL-107, NOAA/Pacific Marine Environmental Laboratory, Seattle, WA, 49 pp.

Plimpton, P.E., H.P. Freitag, and M.J. McPhaden (1997): ADCP velocity from pelagic fish schooling around equatorial moorings. *J. Atmos. Oceanic Tech.*, *14*, 1212–1223.

Plimpton, P.E., H.P. Freitag, and M.J. McPhaden (2000): Correcting moored

ADCP data for fish-bias errors at 0°,110°W and 0°,140°W from 1993 to 1995. NOAA Tech. Memo. OAR PMEL-117, NOAA/Pacific Marine Environmental Laboratory, Seattle, WA, 35 pp.

Pullen, P.E., M.J. McPhaden, H.P. Freitag, and J. Gast (1992): Surface wave induced skew errors in acoustic Doppler current profiler measurements from high shear regimes. In *Proceedings of Oceans '92, Mastering the Oceans Through Technology*, Newport, RI, 26–29 October 1992, 706–711.

RD Instruments (1991): Self-contained acoustic Doppler current profiler (SC-ADCP) technical manual. v–14. (Available from RD Instruments, 9855 Businesspark Ave., San Diego, CA 92131.

Sea-Bird Electronics (1996): Seacat SBE 16-04 Operating Manual, 102 pp. (Available from Sea-Bird Electronics, Inc. 1808 136th Place NE, Bellevue, WA 98005).

Wade, I.P., and K.J. Heywood (2001): Acoustic backscatter observations of zooplankton abundance and behavior and the influence of oceanic fronts in the Northeast Atlantic. *Deep-Sea Res. II*, *48*, 899–924.

Weller, R.A., and R.E. Davis (1980): A vector-measuring current meter. *Deep-Sea Res.*, *27*, 575–582.

Wilson, C.D., and E. Firing (1992): Sunrise swimmers bias acoustic Doppler current profiles. *Deep-Sea Res.*, *39*, 885–892.

Figures

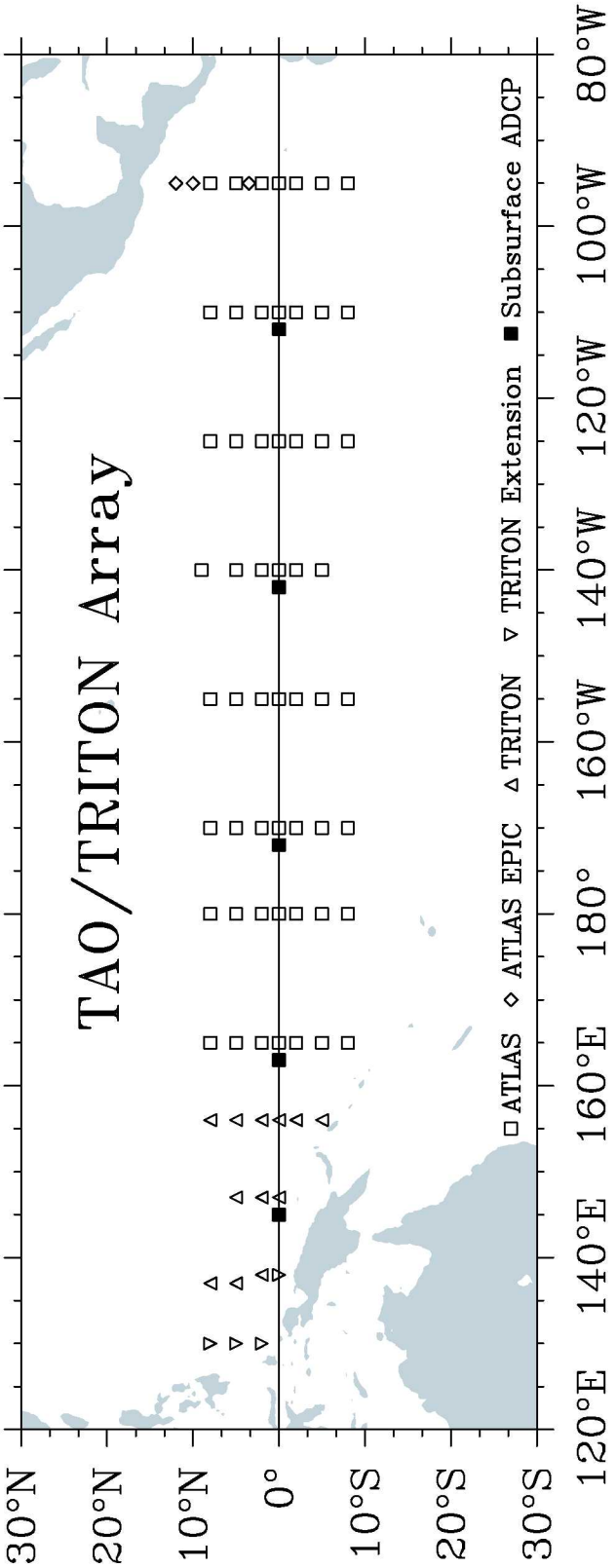

Figure 1: TAO/TRITON array with location of subsurface ADCP moorings maintained jointly by PMEL and JAMSTEC. Also shown are the positions of the surface moorings maintained by PMEL (ATLAS) and by JAMSTEC (TRITON).

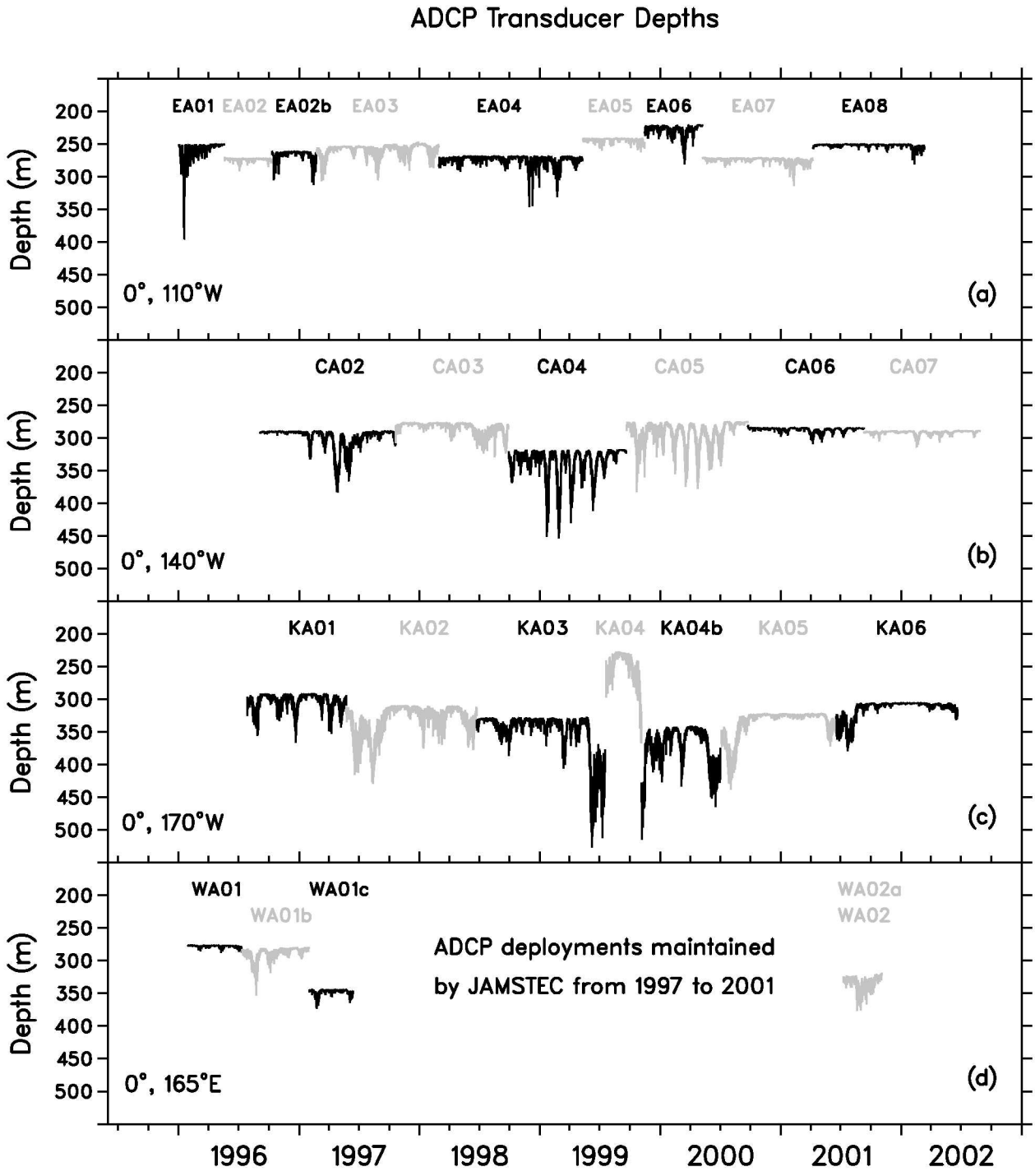

Figure 2: Hourly transducer depths for subsurface ADCP deployments at 0°, 110°W (a), at 0°, 140°W (b), at 0°, 170°W (c), and at 0°, 165°E (d).

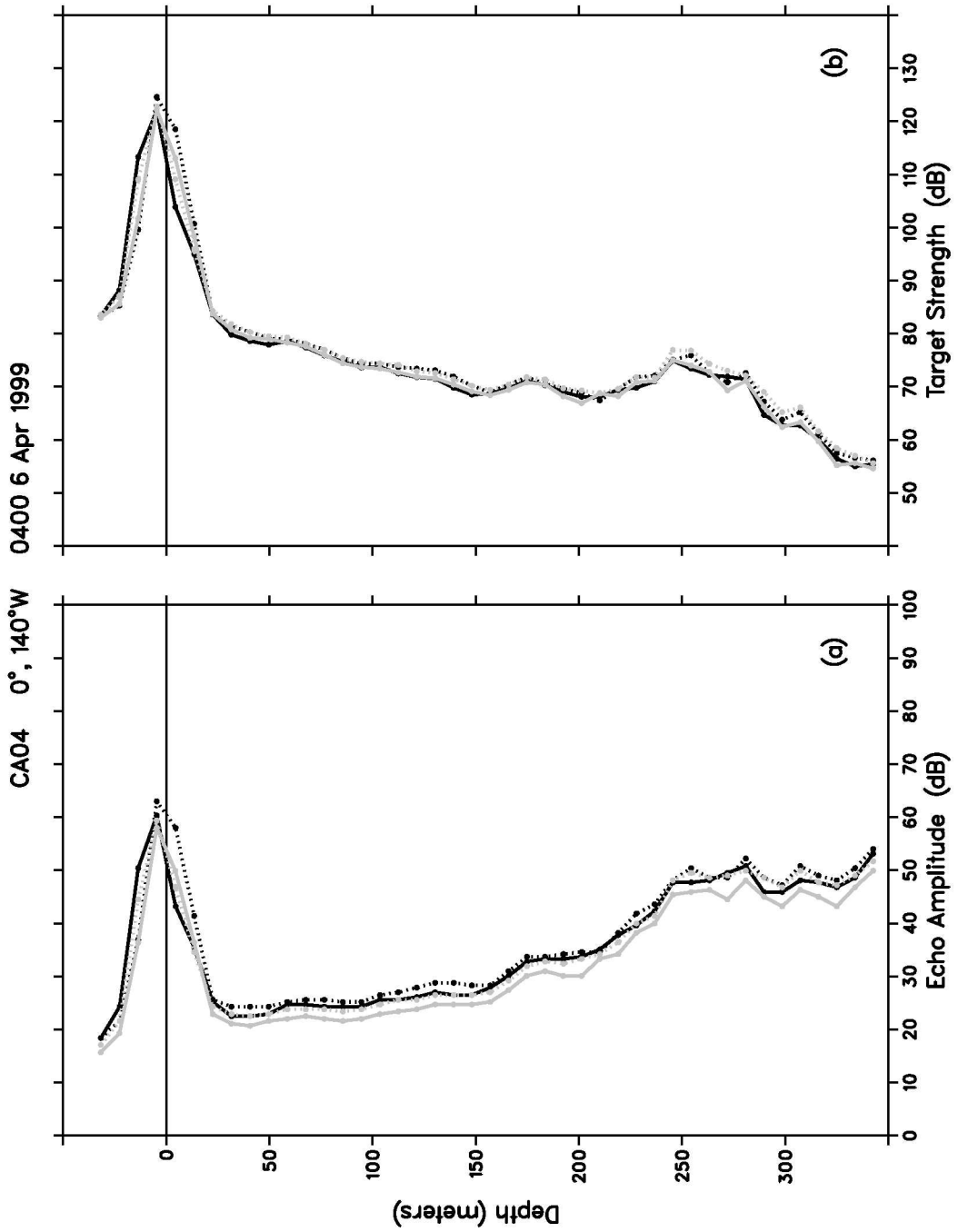

Figure 3: (a) Echo amplitude profiles of the four ADCP beams measured at 0400 on April 6, 1999. (b) Target strength profiles for the four beams computed by adjusting the echo amplitude for the effects of beam spreading and sound absorption. Computing the target strength allows the reflection from the surface to appear as a maximum for over 90% of the hourly profiles. The depth of the bins is relative to the transducer depth indicated by pressure sensors on the mooring.

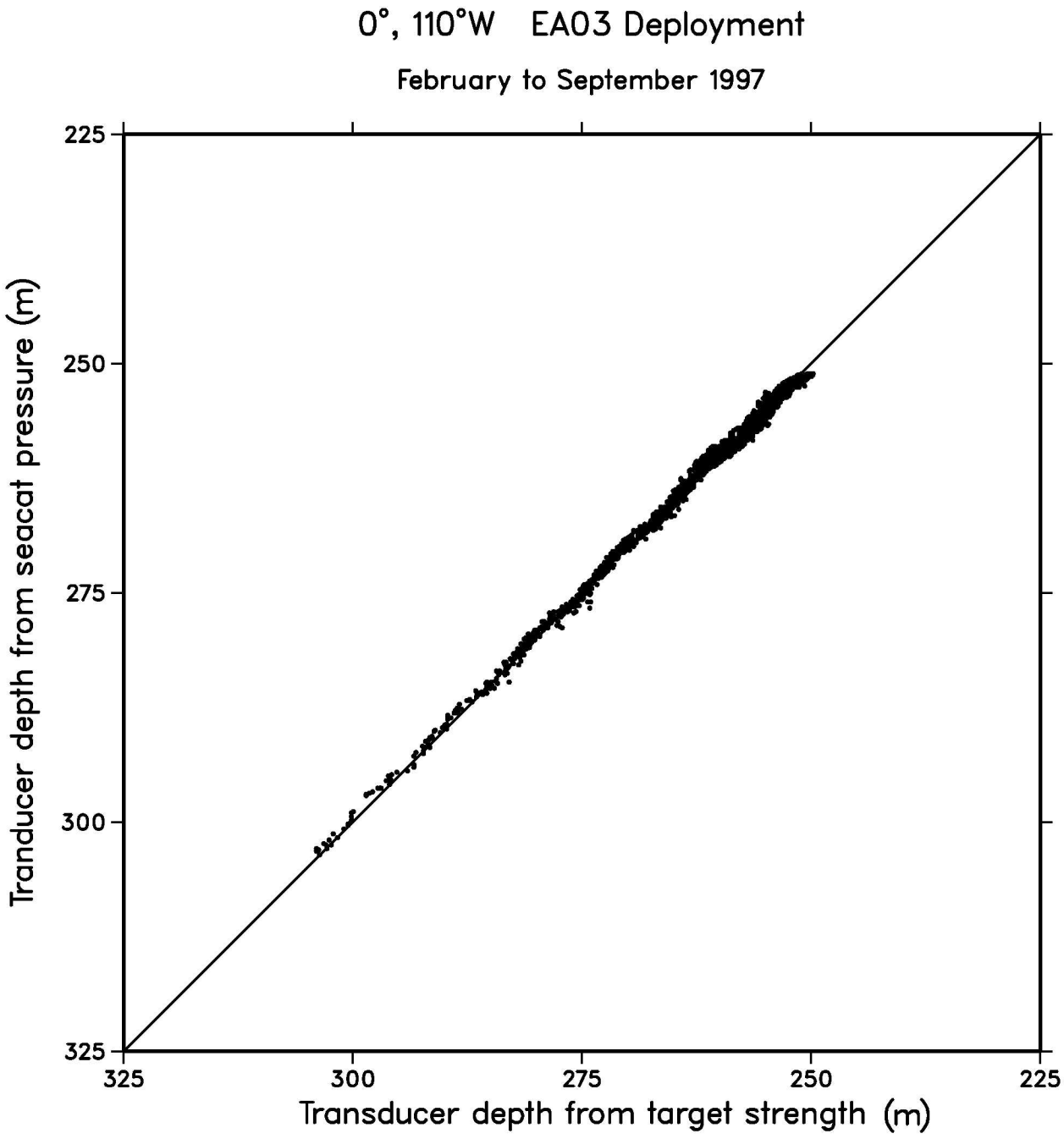

Figure 4: Comparison of the transducer depth determined from target strength and from the Seacat pressure, from February to September, 1997, for the EA03 deployment at 0°, 110°W.

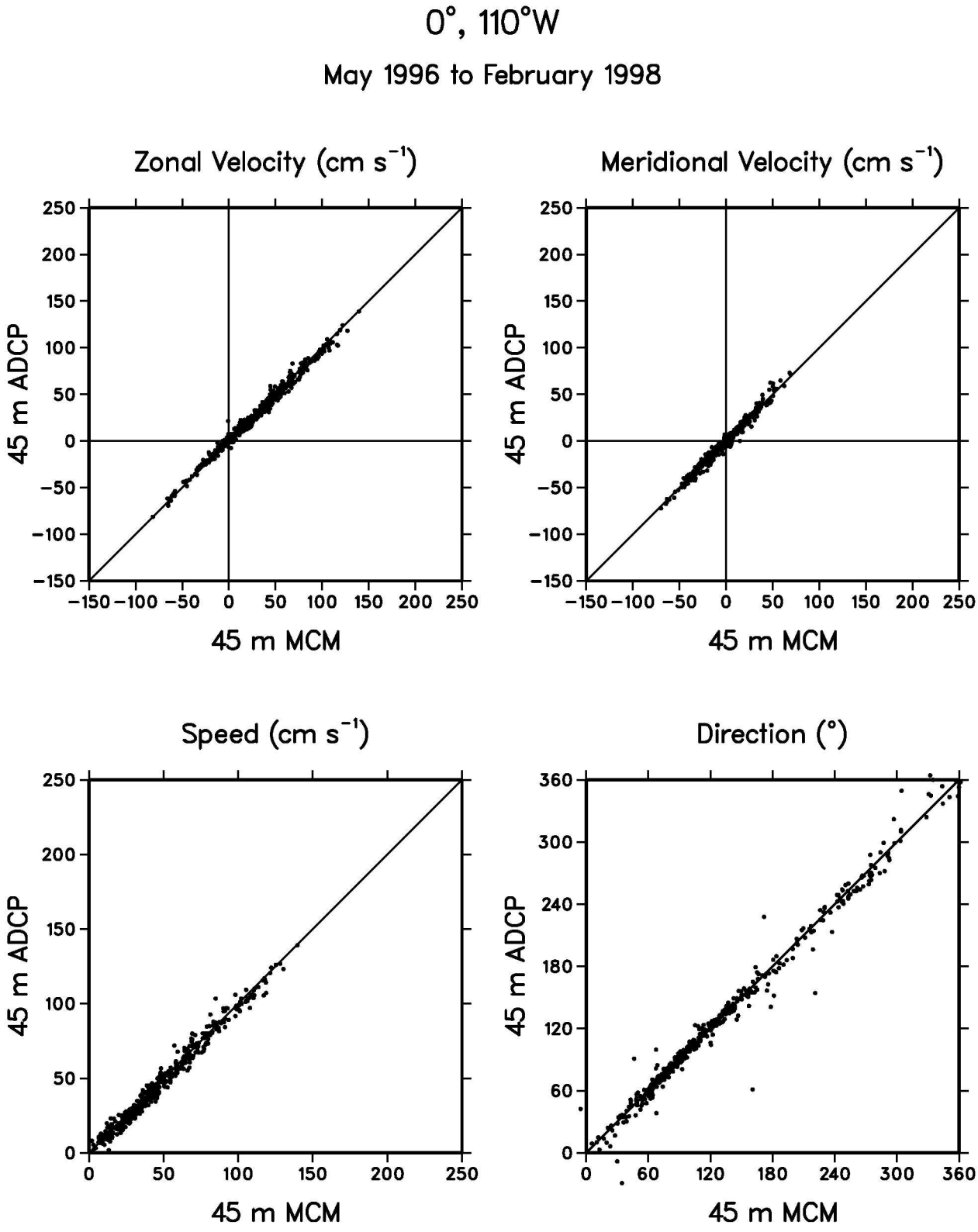

Figure 5: Scatter plot of 45 m daily averaged zonal velocity, meridional velocity, speed, and direction from MCMs and ADCPs measured from May 1996 to February 1998 at 0°, 110°W.

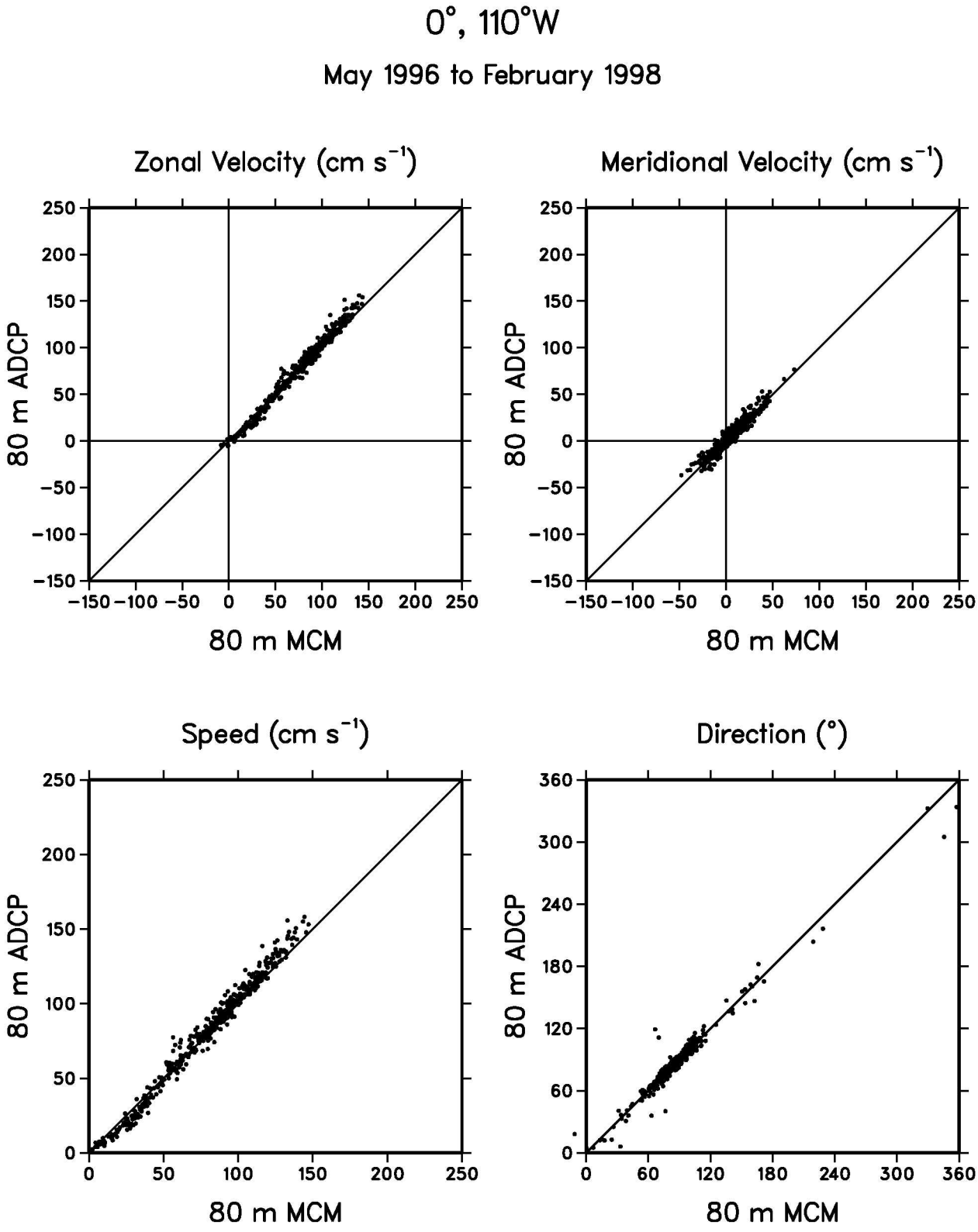

Figure 6: Scatter plot of 80 m daily averaged zonal velocity, meridional velocity, speed, and direction from MCMs and ADCPs measured from May 1996 to February 1998 at 0°, 110°W.

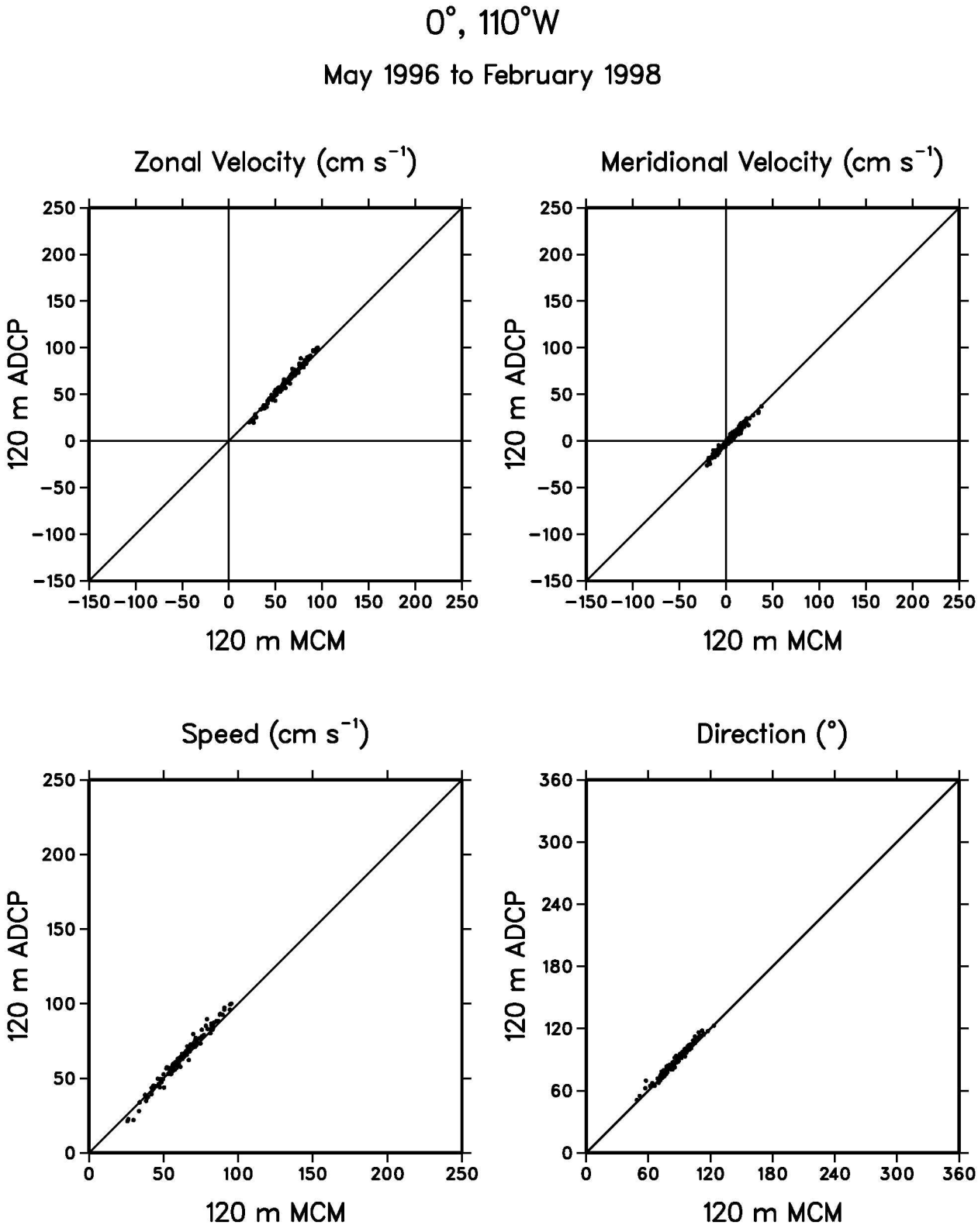

Figure 7: Scatter plot of 120 m daily averaged zonal velocity, meridional velocity, speed, and direction from MCMs and ADCPs measured from May 1996 to February 1998 at 0°, 110°W.

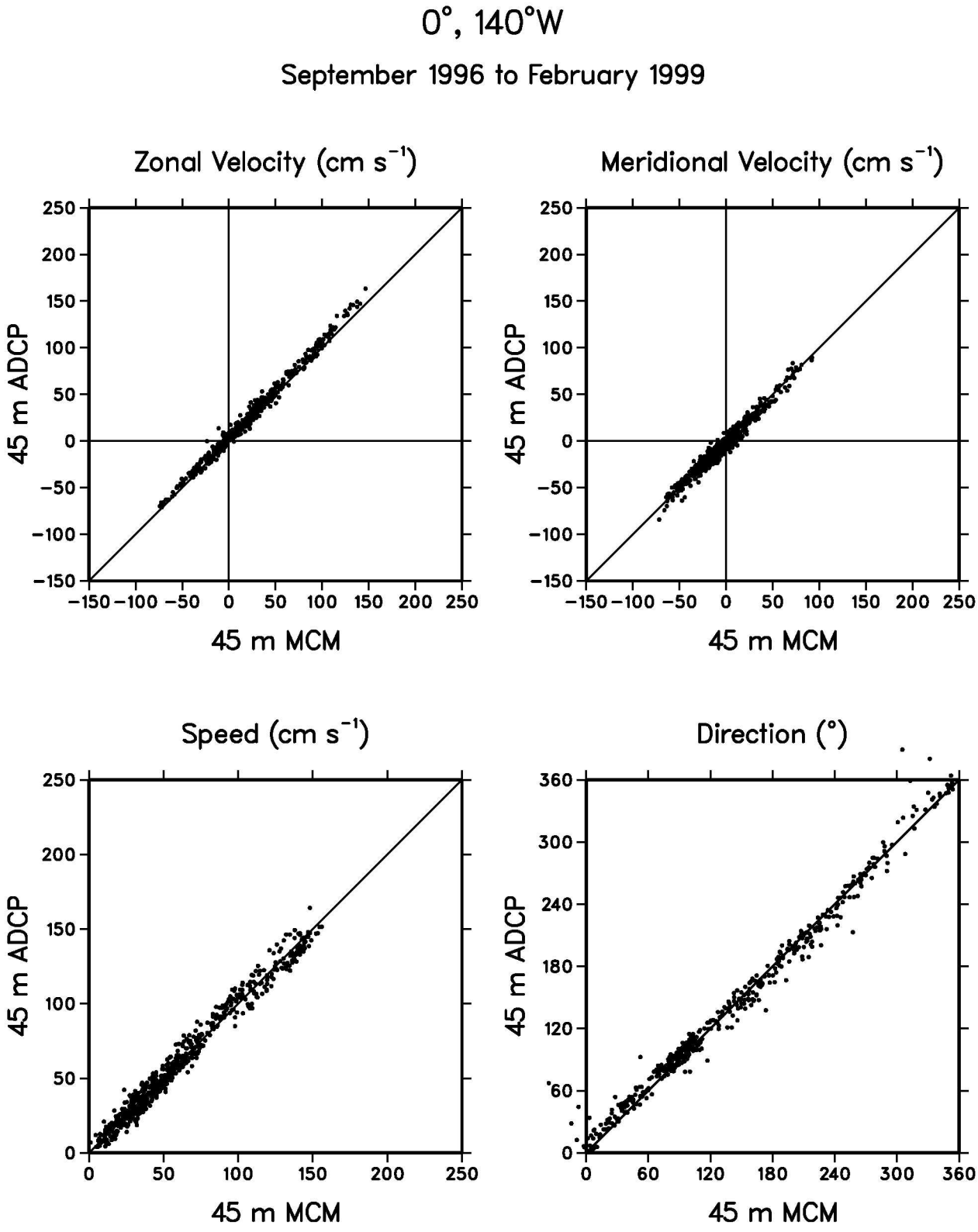

Figure 8: Scatter plot of 45 m daily averaged zonal velocity, meridional velocity, speed, and direction from MCMs and ADCPs measured from September 1996 to February 1999 at 0°, 140°W.

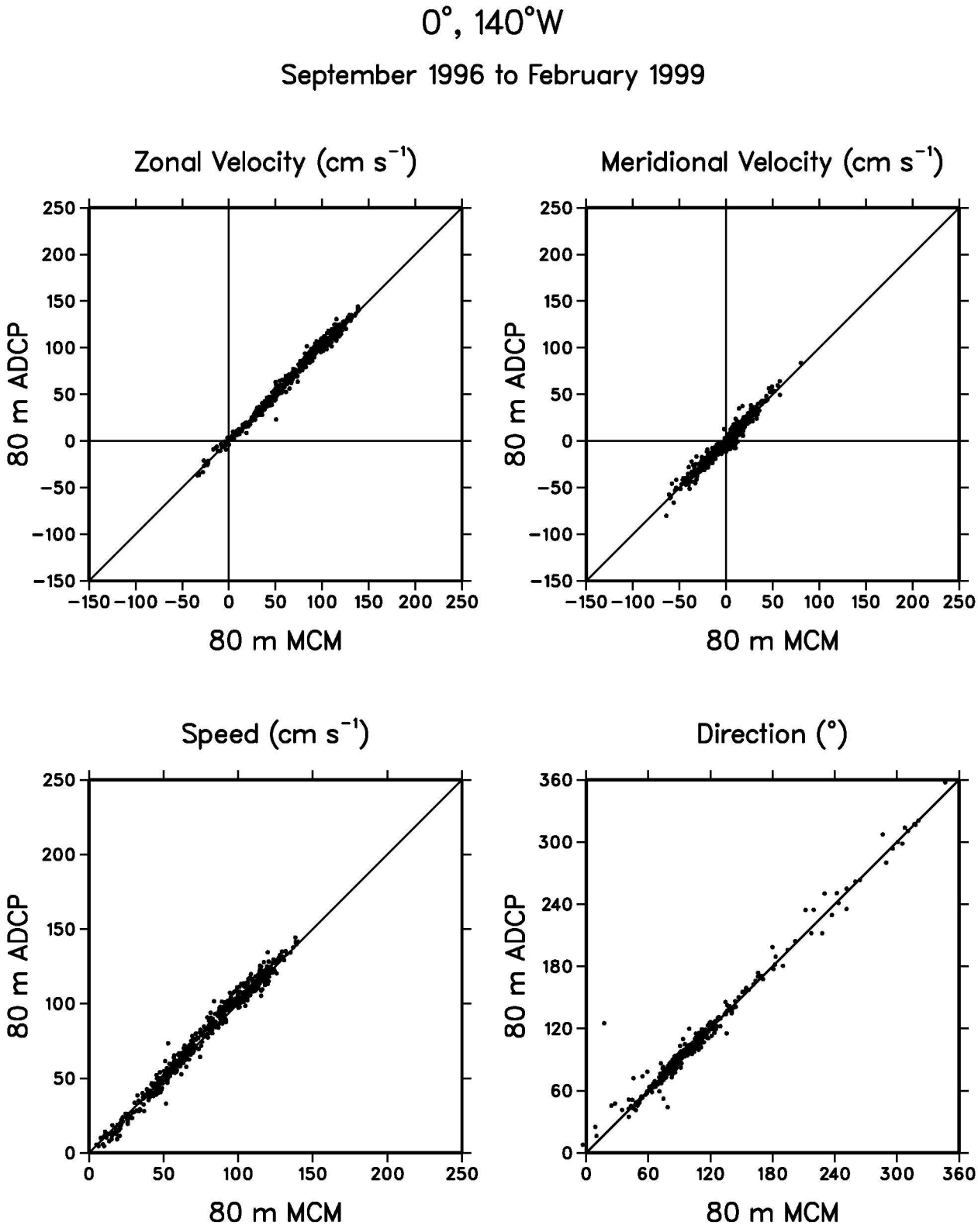

Figure 9: Scatter plot of 80 m daily averaged zonal velocity, meridional velocity, speed, and direction from MCMs and ADCPs measured from September 1996 to February 1999 at 0°, 140°W.

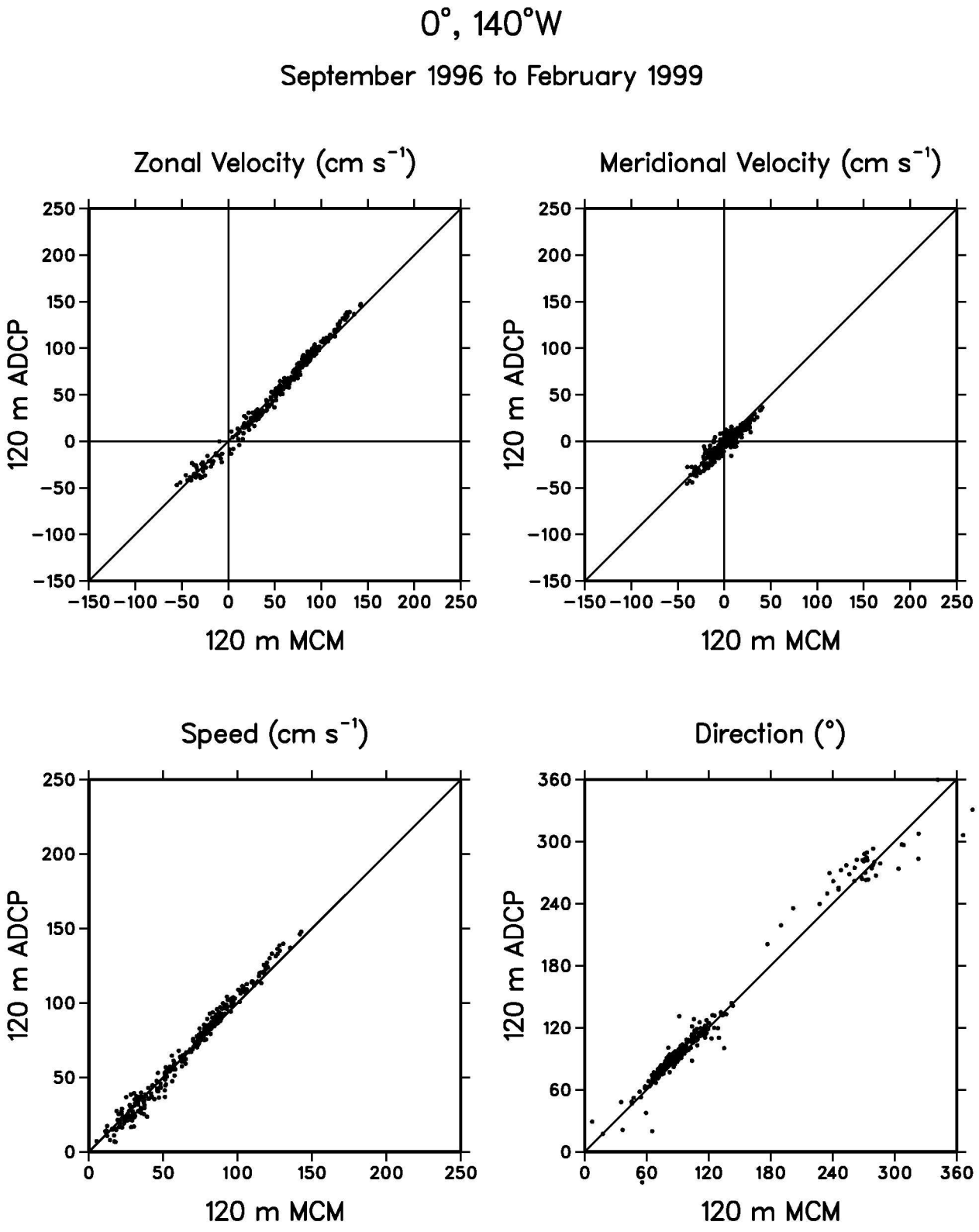

Figure 10: Scatter plot of 120 m daily averaged zonal velocity, meridional velocity, speed, and direction from MCMs and ADCPs measured from September 1996 to February 1999 at 0°, 140°W.

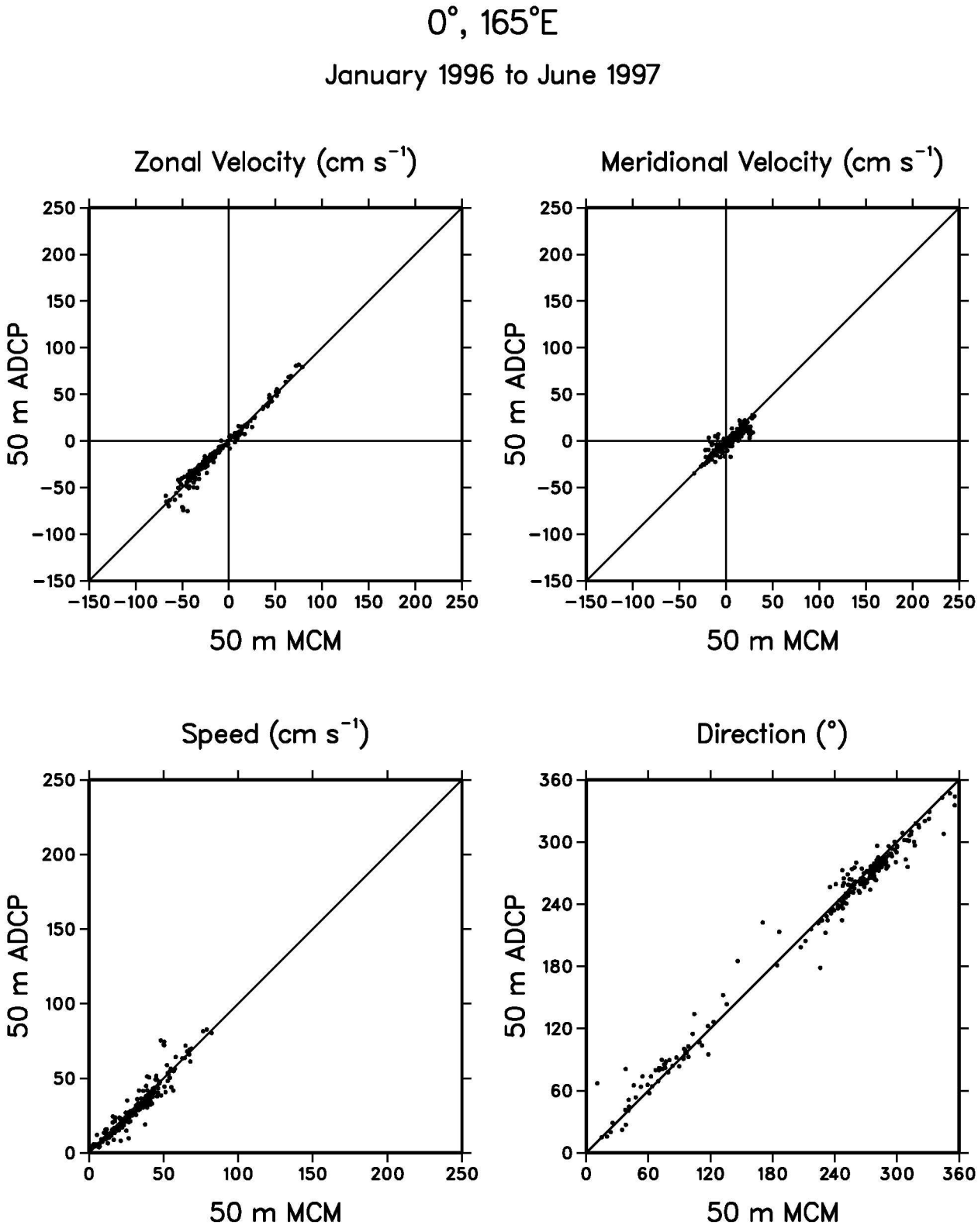

Figure 11: Scatter plot of 50 m daily averaged zonal velocity, meridional velocity, speed, and direction from MCMs and ADCPs measured from January 1996 to June 1997 at 0°, 165°E.

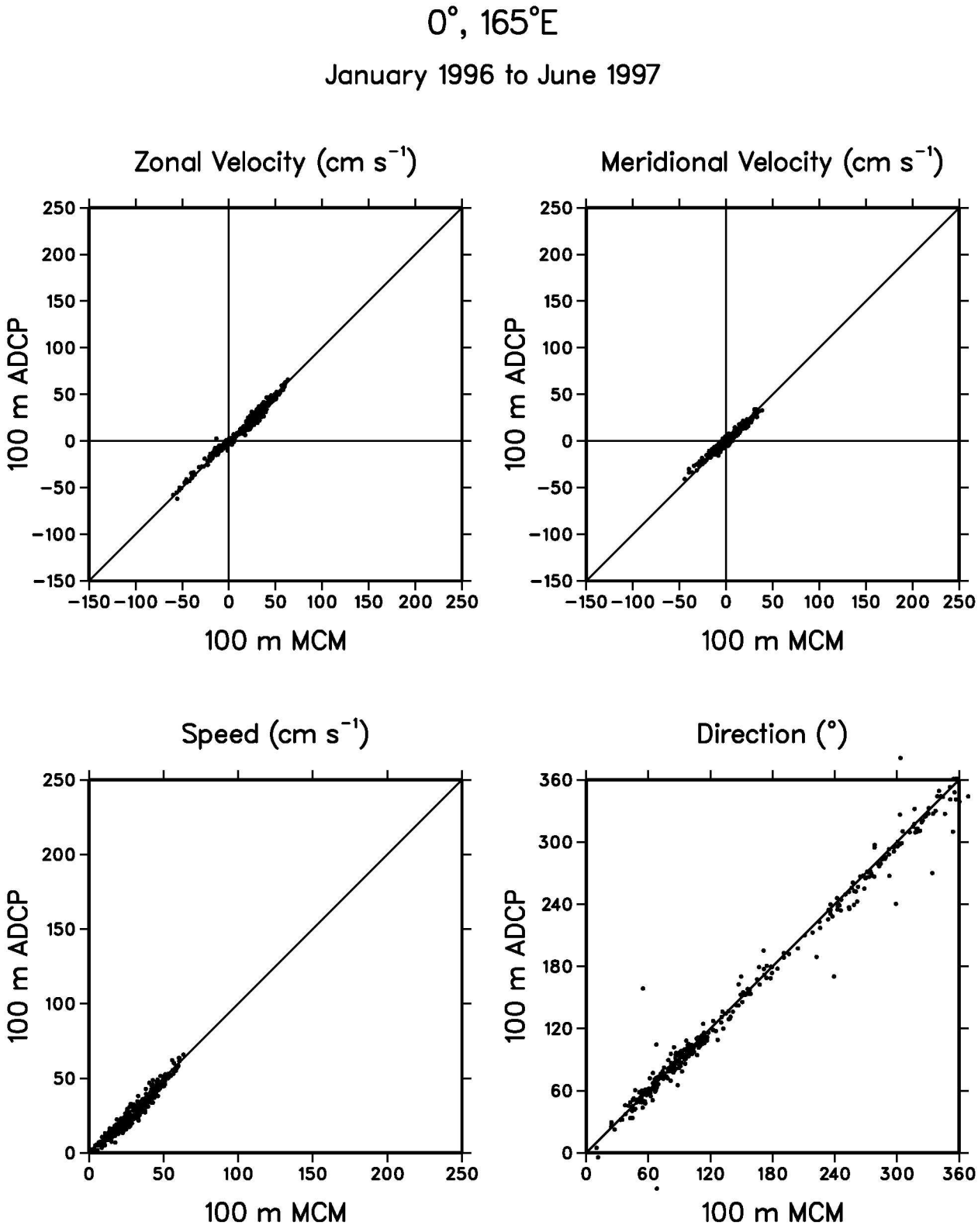

Figure 12: Scatter plot of 100 m daily averaged zonal velocity, meridional velocity, speed, and direction from MCMs and ADCPs measured from January 1996 to June 1997 at 0°, 165°E.

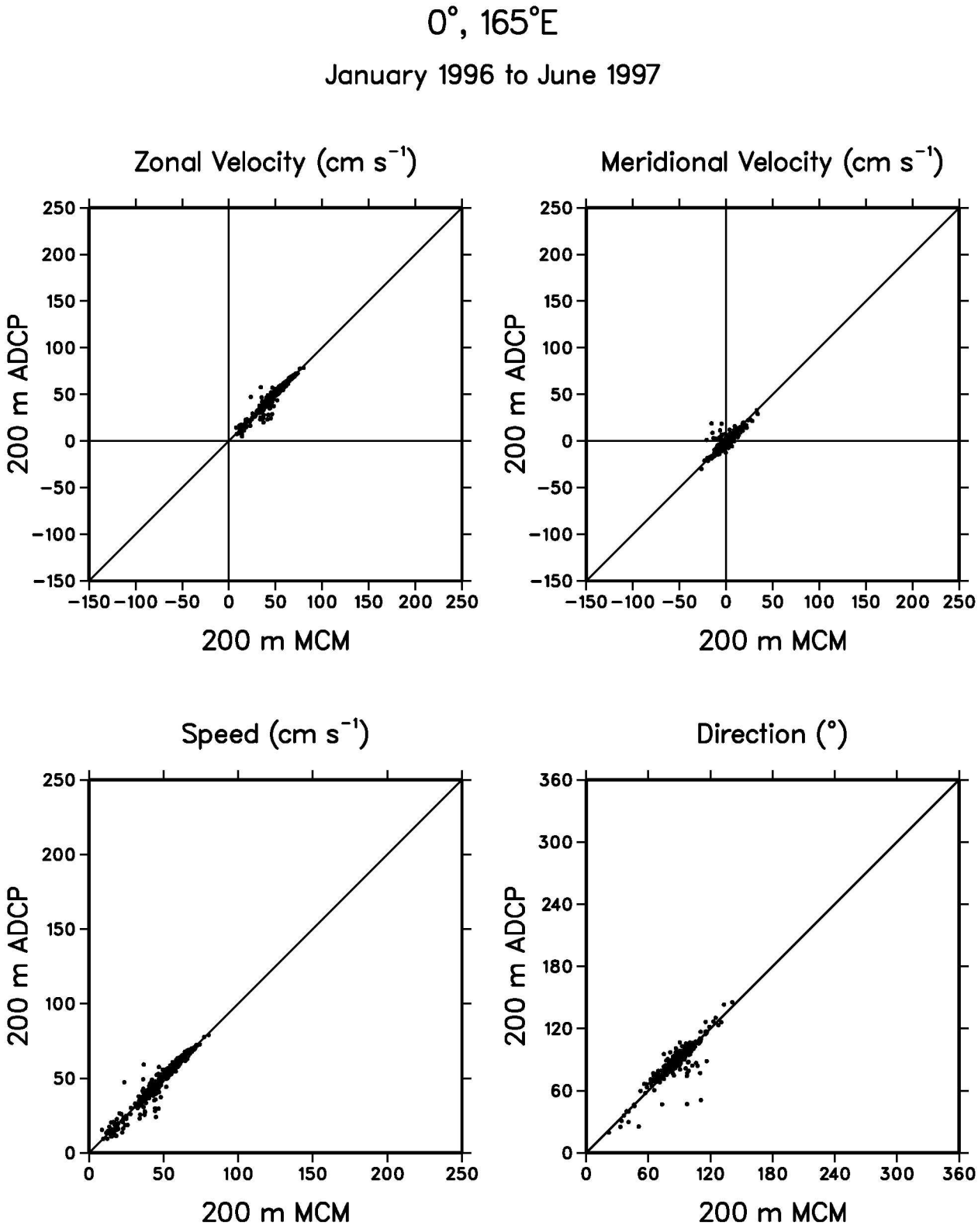

Figure 13: Scatter plot of 200 m daily averaged zonal velocity, meridional velocity, speed, and direction from MCMs and ADCPs measured from January 1996 to June 1997 at 0°, 165°E.

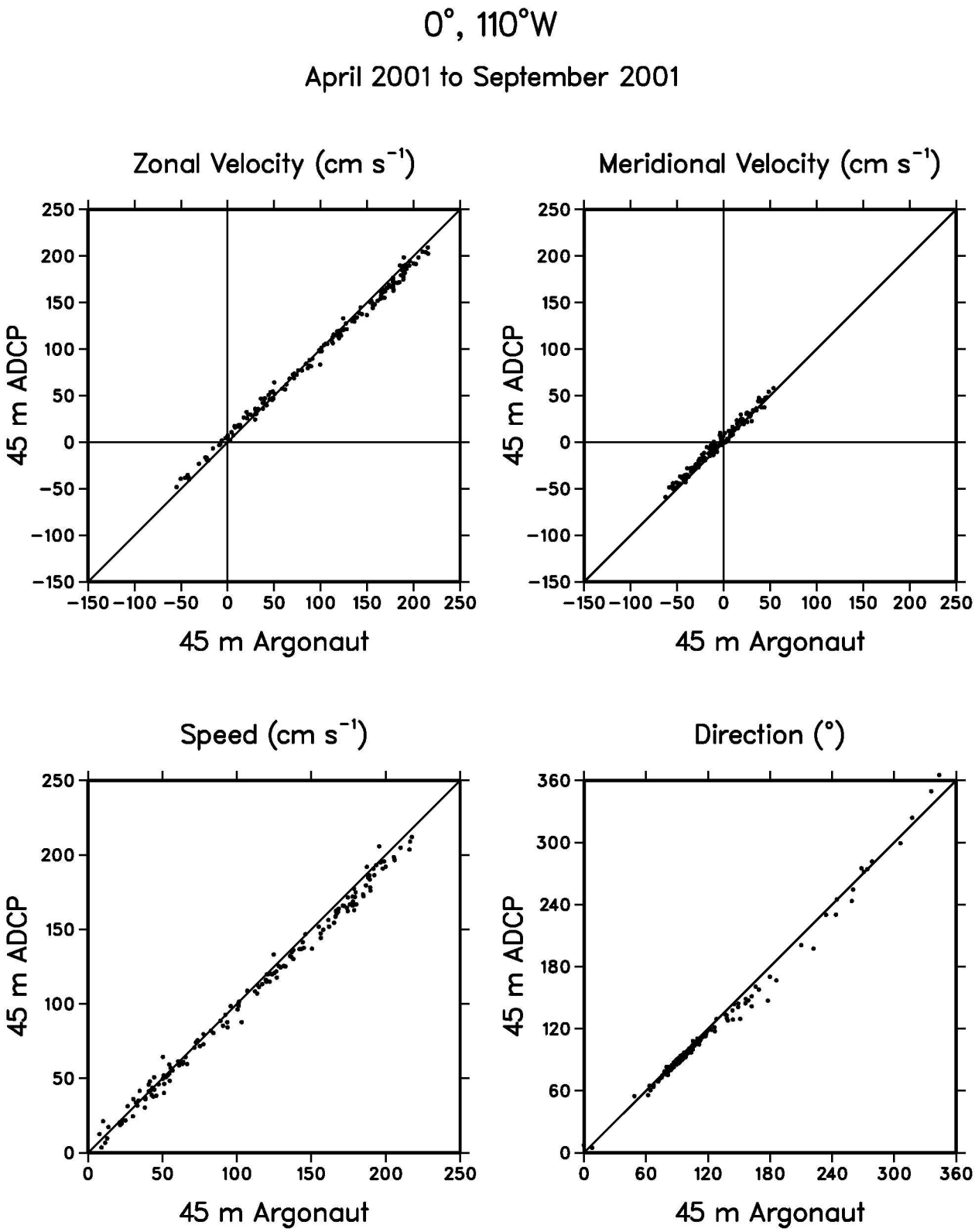

Figure 14: Scatter plot of 45 m daily averaged zonal velocity, meridional velocity, speed, and direction from Sontek Argonaut-MD current meters and ADCPs measured from April to September 2001 at 0°, 110°W.

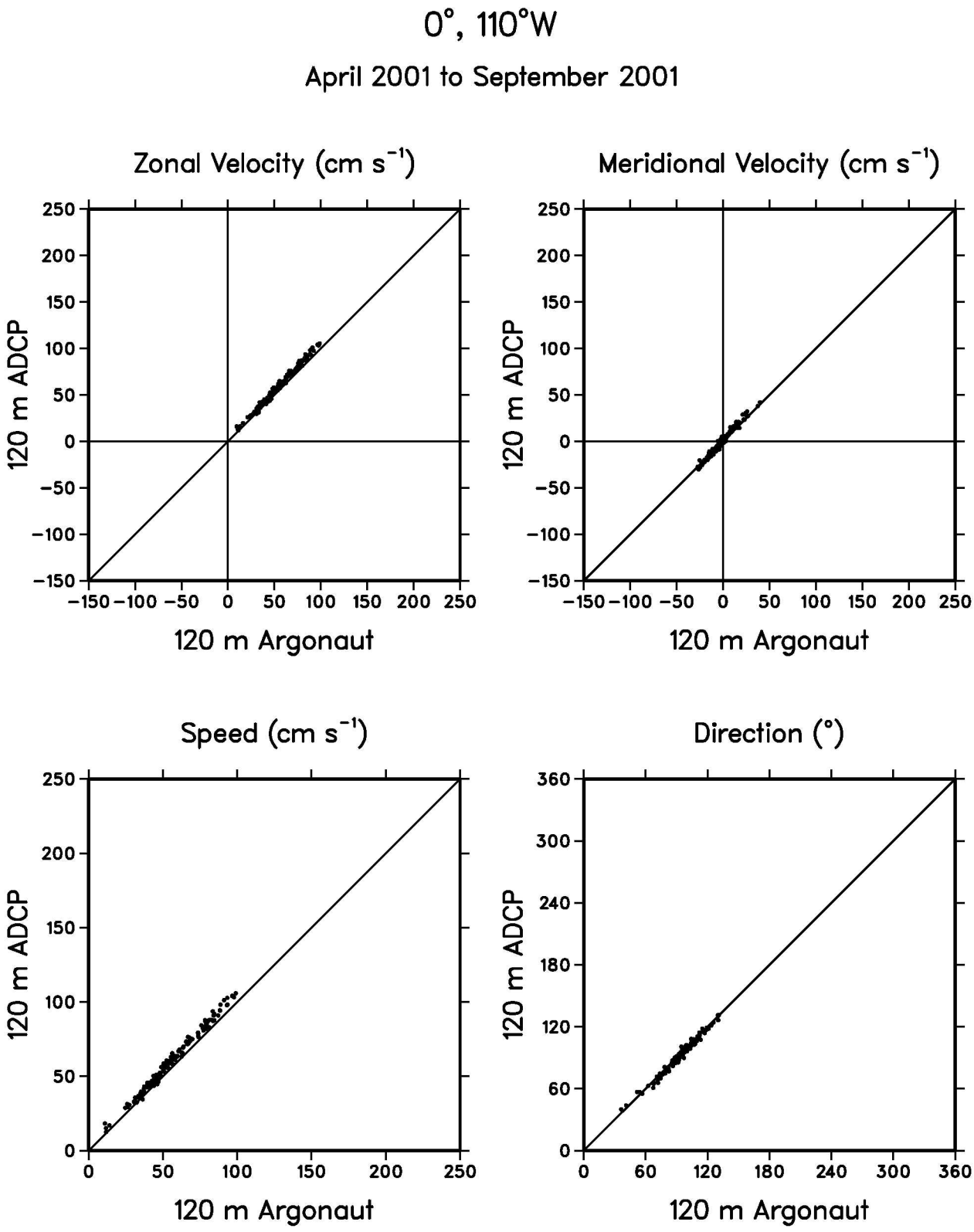

Figure 15: Scatter plot of 120 m daily averaged zonal velocity, meridional velocity, speed, and direction from Sontek Argonaut-MD current meters and ADCPs measured from April to September 2001 at 0°, 110° W.

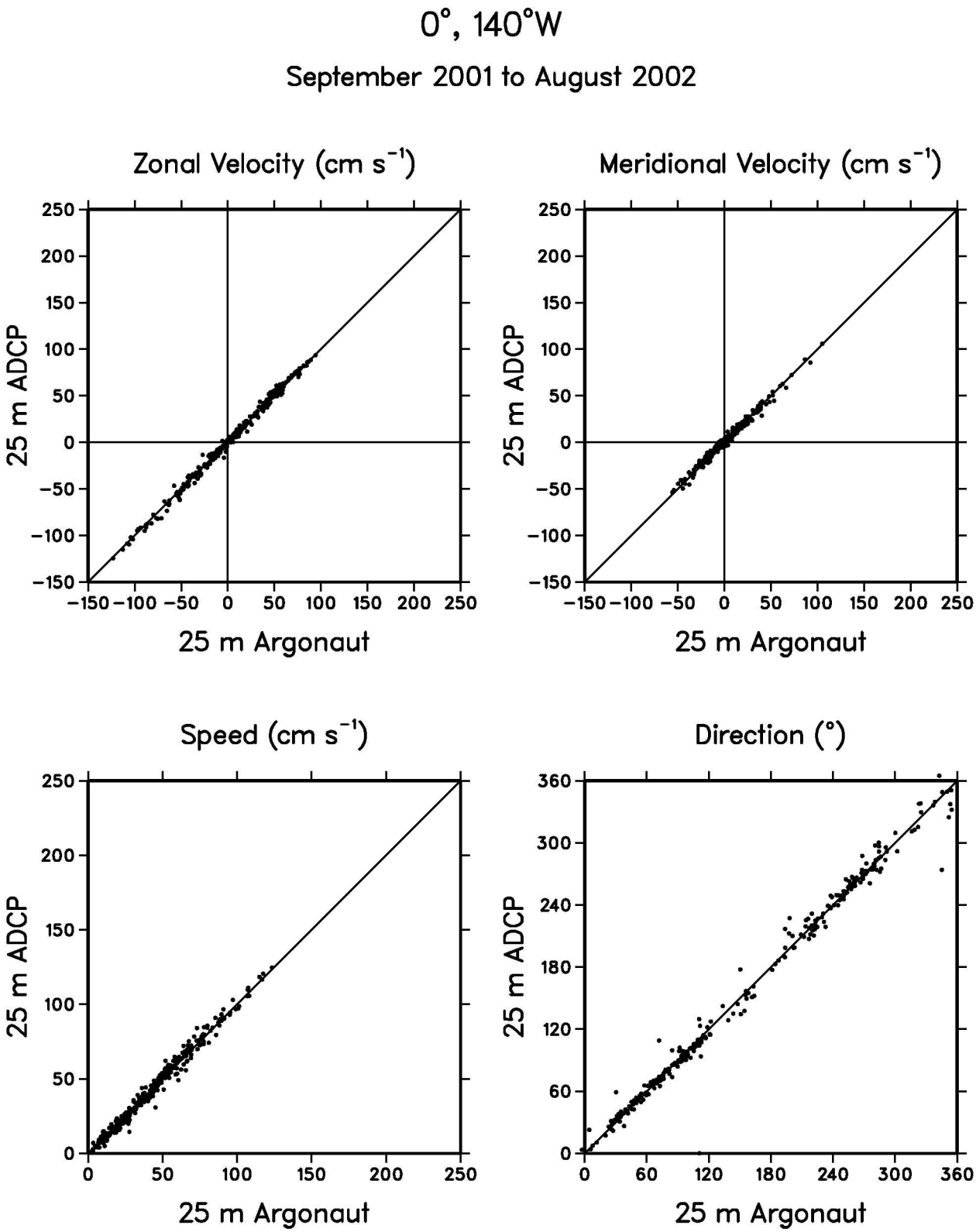

Figure 16: Scatter plot of 25 m daily averaged zonal velocity, meridional velocity, speed and direction from Sontek Argonaut-MD current meters and ADCPs measured from September 2001 to August 2002 at 0°, 140°W. The 25 m ADCP data are computed by extrapolation from the two shallowest good ADCP values before mapping to 5-m standard depths.

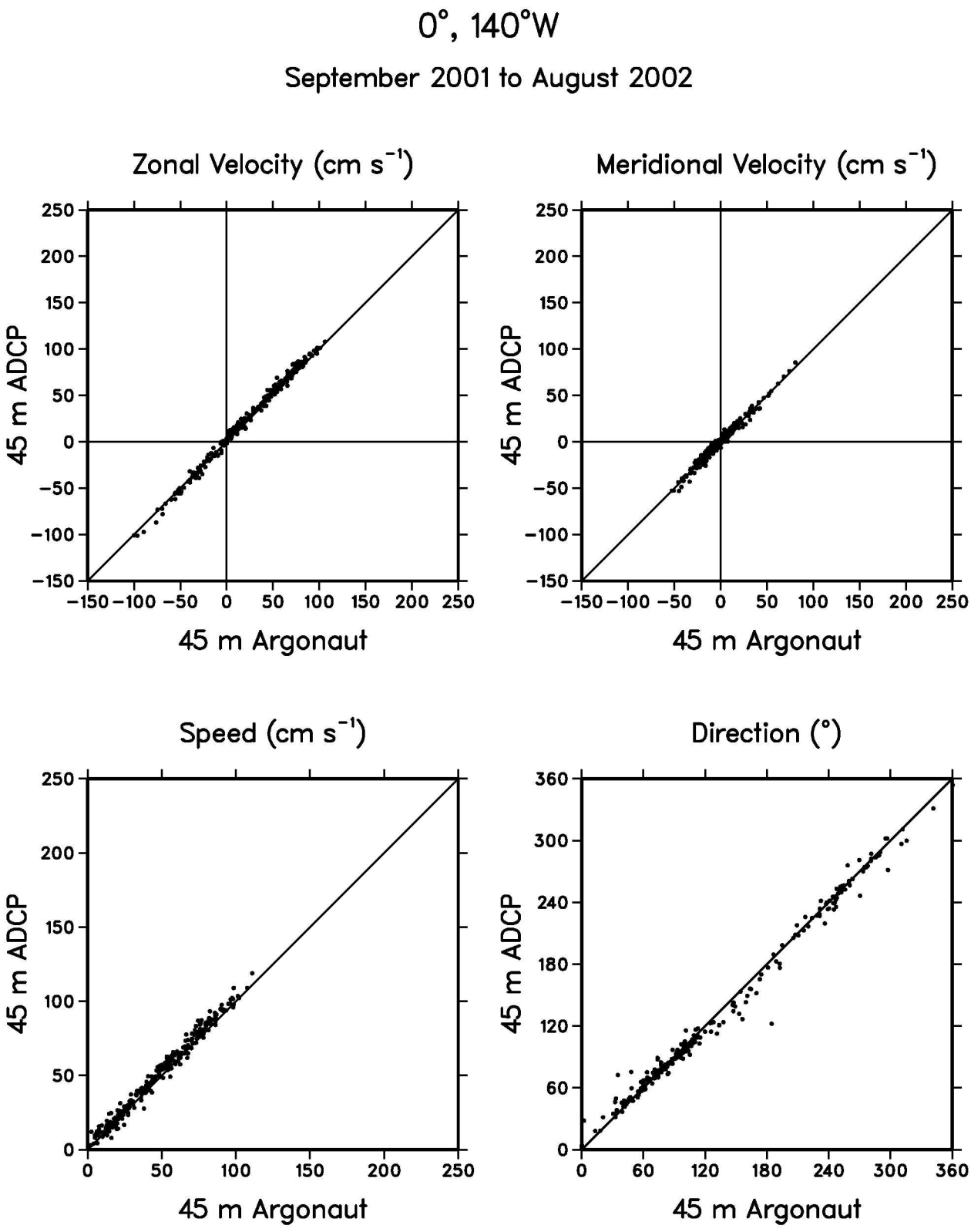

Figure 17: Scatter plot of 45 m daily averaged zonal velocity, meridional velocity, speed and direction from Sontek Argonaut-MD current meters and ADCPs measured from September 2001 to August 2002 at 0°, 140°W.

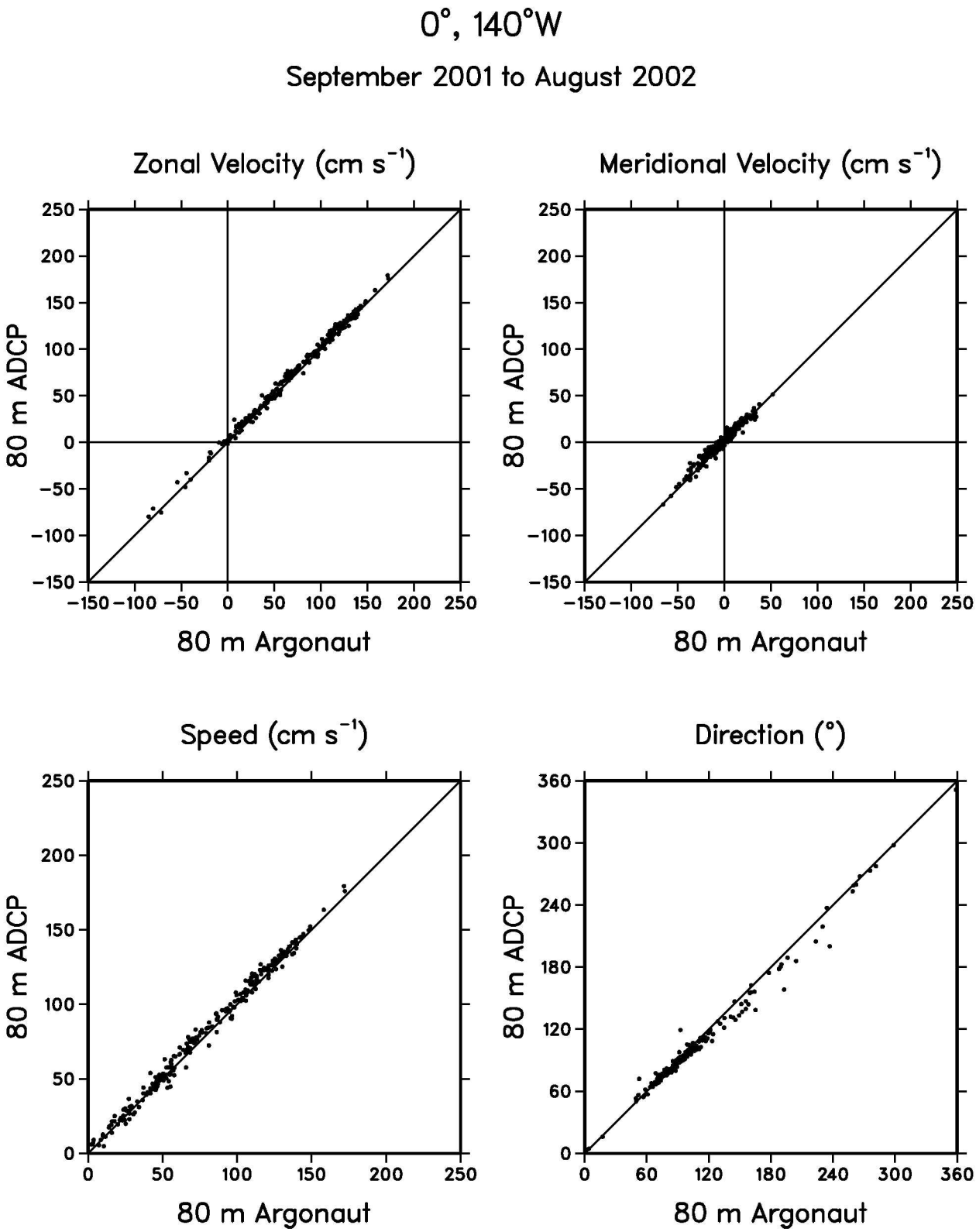

Figure 18: Scatter plot of 80 m daily averaged zonal velocity, meridional velocity, speed, and direction from Sontek Argonaut-MD current meters and ADCPs measured from September 2001 to August 2002 at 0°, 140°W.

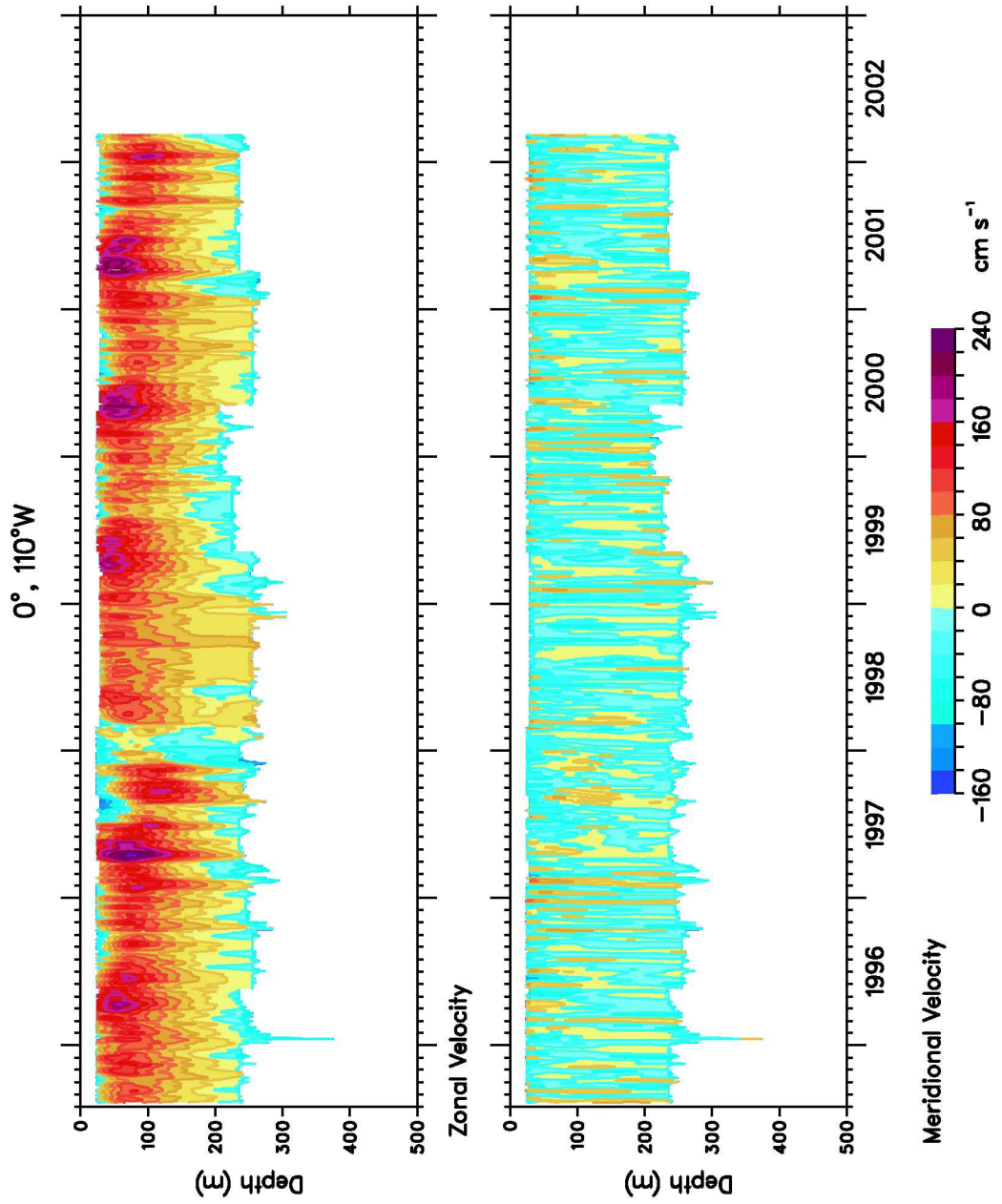

Figure 19: Contour plot of daily averaged zonal and meridional ADCP velocity at 0°, 110°W.

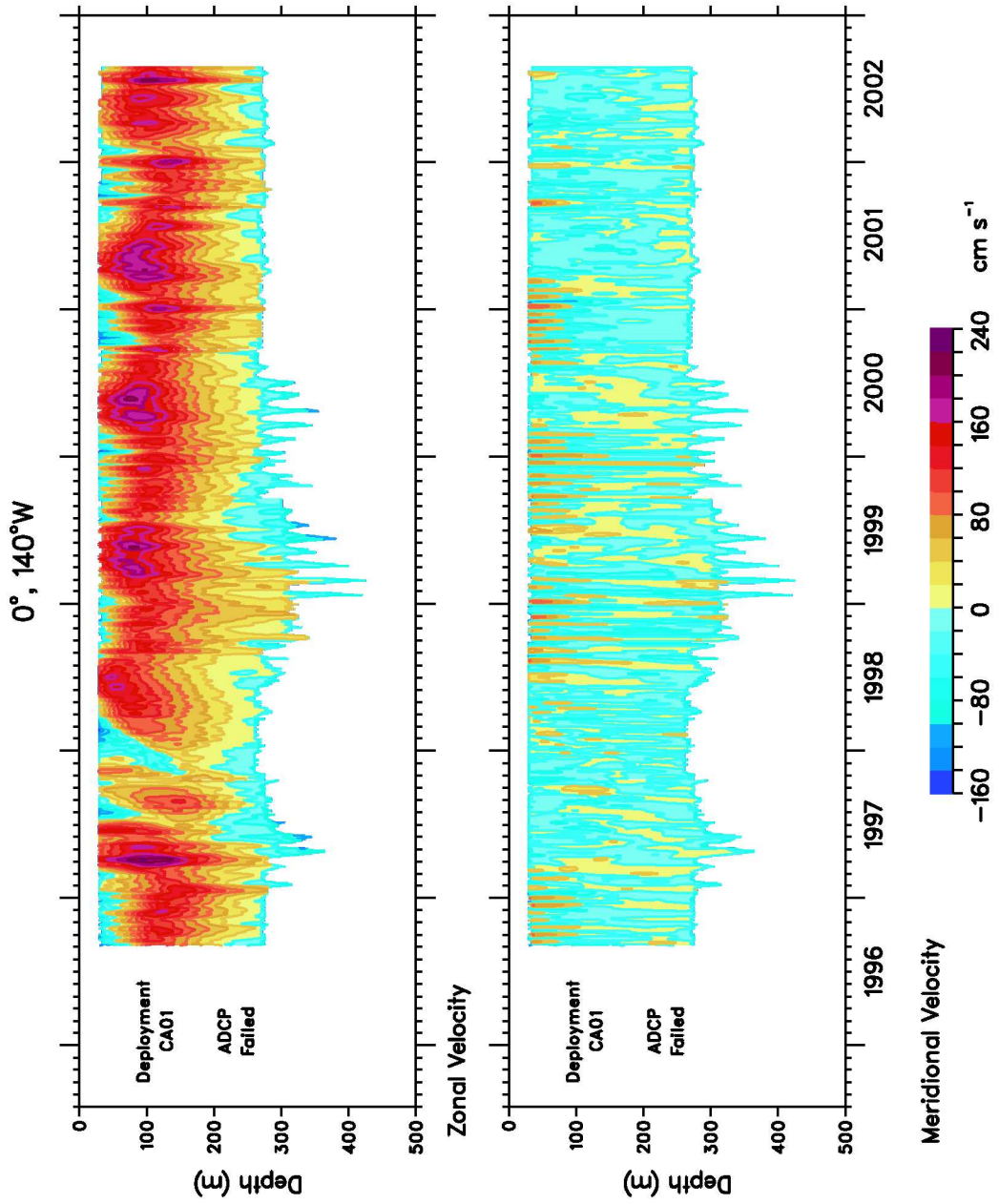

Figure 20: Contour plot of daily averaged zonal and meridional ADCP velocity at 0°, 140°W.

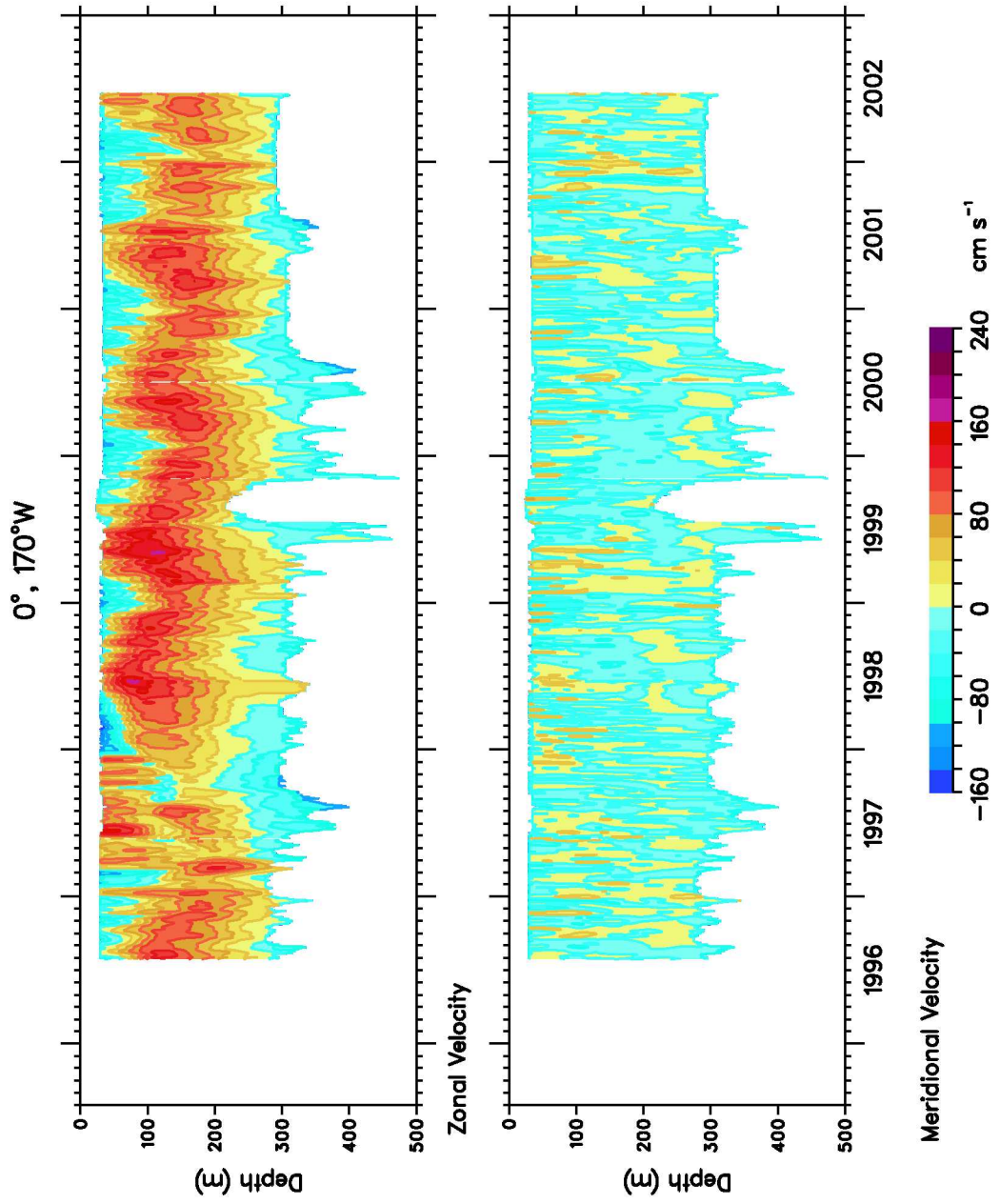

Figure 21: Contour plot of daily averaged zonal and meridional ADCP velocity at 0°, 170°W.

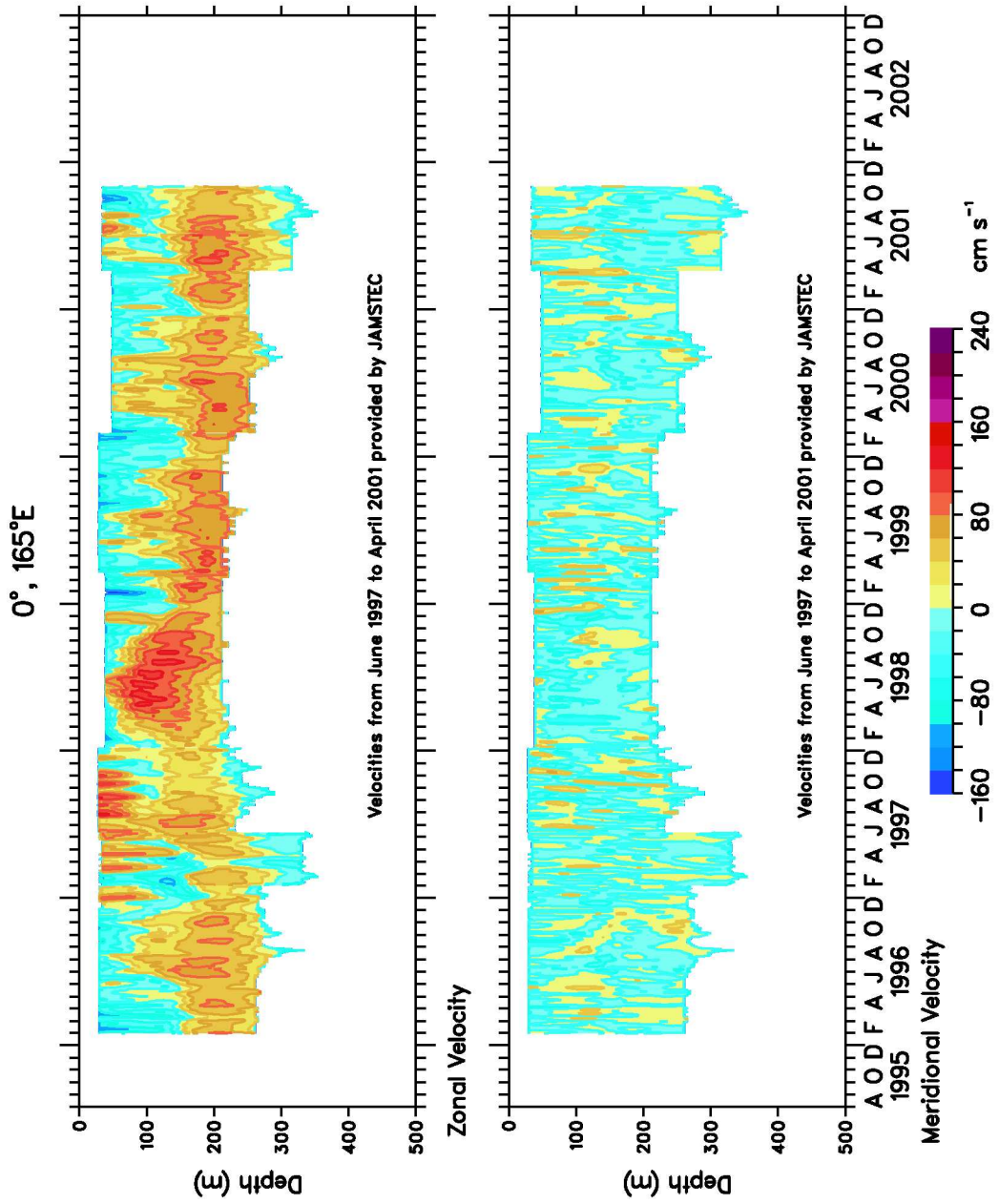

Figure 22: Contour plot of daily averaged zonal and meridional ADCP velocity at 0°, 165°E.

Appendix 1: Computation of target strength from the ADCP echo amplitude

The RDI ADCP acoustic signal is scattered by suspended matter in the ocean and by the sea surface. The mean volume backscatter of the ADCP has been related to the abundance and distribution of scatterers (Flagg and Smith, 1989; Wade and Heywood, 2001). In order to calculate an absolute backscatter value from the echo amplitude, the ADCP must be calibrated. The calibration, performed at RDI's factory, determines transducer characteristics such as power into the water, system noise factors, a reference thermal noise for the electronics and the transducer temperature during calibration. In addition, power attenuation due to propagation losses such as absorption and beam spreading must be included. However, to locate the position of the maximum reflection of the sea surface from the echo amplitude, only the relative, not the absolute, backscatter strength is needed. Therefore, the PMEL ADCPs have not been calibrated for absolute backscatter and, when needed, nominal values, which are independent of depth, are used in the equation for backscatter strength.

The backscatter value, or target strength, is determined from the ADCP echo amplitude by the following equation (RD Instruments, 1991).

$$\mathrm{Sv} = 10\log_{10}\left(\frac{4.47\times10^{-20}\ \mathrm{K2\ Ks\ (Tx}+273.18)(10^{\mathrm{Kc(Ea-Er)}/10}-1)\ \mathrm{R}^2}{\mathrm{c\ P\ K1}\ 10^{-2\mathrm{eR}/10}}\right) \tag{1}$$

where

Tx	is the temp of transducer (°C)
R	is the range along beam to scatterers (m)
e	is the absorption coefficient of water (dB/m)
P	is the transmit pulse length (m)
c	is the speed of sound at the scattering layer being measured (m/s)
K1	is the power into the water (watts)
Ea	is the echo amplitude in counts
Er	is the reference thermal noise of ADCP electronics (counts)
Kc	is the conversion factor for echo amplitude (dB/counts)
K2	is the system noise factor
Ks	is the system constant dependent on ADCP frequency

Values used for the variables in equation (1) are:

K2	=	3.6, the nominal value for a 153.6 kHz system
Ks	=	4.17×10^5
P	=	8.68 m the nominal pulse length for a 20 degree system
Kc	=	$127.3/(\mathrm{Tx}+273.18)$

The temperature measured by the ADCP temperature probe was used for

Tx, the temperature of the transducer. Average historical sound speed profiles were used for c, the speed of sound at the scattering layer.

The power into the water was estimated by

$$\mathrm{K1} = ((\mathrm{Vs} \times \mathrm{a}) - \mathrm{b})/\mathrm{c1})2 \times \mathrm{K1c} \tag{2}$$

where

$$\begin{aligned} \mathrm{a} &= .17 \text{ for } 153.6 \text{ kHz system} \\ \mathrm{b} &= 5.767 \text{ for } 153.6 \text{ kHz system} \\ \mathrm{c1} &= 34.247 \text{ for } 153.6 \text{ kHz system} \\ \mathrm{K1c} &= 3.9 \text{ watts, the nominal value for } 153 \text{ kHz} \end{aligned}$$

Vs is the high voltage value. Although hourly voltage values are available, they are not depth dependent so a mean voltage for the deployment was used. Voltage was converted into counts by

$$\mathrm{Vs(volts)} = .17 * \mathrm{Vs(counts)} \tag{3}$$

The slant range R was computed by

$$\mathrm{R} = \left(\frac{\mathrm{Blnk} + \mathrm{abs}(\mathrm{P} - \mathrm{BW})/2 + (\mathrm{N} * \mathrm{BW}) + (\mathrm{BW}/4)}{\cos(\theta)} \right) \left(\frac{\mathrm{c}'}{1475.1} \right) \tag{4}$$

where

$$\begin{aligned} \theta &= 20 \text{ degree, the ADCP beam angle} \\ \mathrm{Blnk} &= 4.34 \text{ m, the nominal blanking set for the ADCP} \\ \mathrm{P} &= 8.68 \text{ m, the nominal pulse length} \\ \mathrm{BW} &= 8.68 \text{ m, the nominal bin width} \\ \mathrm{N} &= \text{bin number} \\ \mathrm{c}' &= \text{mean sound speed between the transducer depth and the depth of the bin, determined from average historical sound speed profiles.} \end{aligned}$$

The BW/4 factor was included because the ADCP samples the echo amplitude in the last quarter of each depth cell.

Equations to calculate absorption in seawater, established by Francois and Garrison (1982), were used assuming a pH value of 8.1 and temperature and salinity values from average historical CTD data (Appendix 2). The absorption coefficient, e, ranged from .048 dB/m at depth to .064 dB/m near the surface.

The reference thermal noise (Er) was not available without instrument calibration. However, this parameter was estimated for each beam by averaging the echo amplitude of the four bins furthest from the transducer (with a range greater than the surface of the water). For these bins, propagation losses have reduced the echo amplitude counts to a minimum value, which approximates the reference noise of the instrument.

Appendix 2: Calculation of sound absorption

The Francois and Garrison (1982) equation for the absorption of sound in seawater gives the absorption as the sum of contributions from boric acid (BA), magnesium sulfate (MS) and pure water (PW). Thus

$$\text{Absorption} = (\text{BA} + \text{MS} + \text{PW})/1000 \quad \text{dB/m}$$

The sum of the contributions is divided by 1000 to convert dB/km to dB/m.

Temperature (T in °C), salinity (S) and sound velocity (SndV) are determined from historical conductivity/temperature/depth (CTD) data. The pH was set to 8.1 and the frequency (freq) of the ADCP is 153.6 kHz. D is depth.

Boric acid contribution:

$$\text{BA} = \text{A}_1 * \text{P}_1 * \text{f}_1 * \text{freq}^2/(\text{freq}^2 + \text{f}_1^2)$$

where

$$\begin{aligned} \text{A}_1 &= 8.86\ (10^{(0.78*\text{pH}-5)})/\text{SndV} \\ \text{P}_1 &= 1 \\ \text{f}_1 &= 2.8(\text{S}/35)^{.5}\ 10^{(4-1245/(273.18+\text{temp}))} \end{aligned}$$

$MgSO_4$ contribution:

$$\text{MS} = (\text{A}_2 * \text{P}_2 * \text{f}_2 * \text{freq}^2)/(\text{freq}^2 + \text{f}_2^2)$$

where

$$\begin{aligned} \text{A}_2 &= 21.44\ \text{S}\ (1 + 0.025\ \text{T})/\text{SndV} \\ \text{P}_2 &= 1 - 1.37 \times 10^{-4}\ \text{D} + 6.2 \times 10^{-9}\ \text{D}^2 \\ \text{f}_2 &= 8.17 \times 10^{(8-1990/(273.18+\text{T}))})/(1 + 0.0018(\text{S} - 35)) \end{aligned}$$

Pure water contribution:

$$\text{PW} = \text{A}_3\text{P}_3\text{freq}^2$$

where

$$\text{P}_3 = 1 - 3.83 \times 10^{-5}\ \text{D} + 4.9 \times 10^{-10}\ \text{D}^2$$

For temperatures less than or equal to 20°C:

$$\text{A}_3 = 4.937 \times 10^{-4} - 2.59 \times 10^{-5}\ \text{T} + 9.11 \times 10^{-7}\ \text{T}^2 - 1.50 \times 10^{-8}\ \text{T}^3$$

For temperatures greater than 20°C:

$$\text{A}_3 = 3.964 \times 10^{-4} - 1.146 \times 10^{-5}\ \text{T} + 1.45 \times 10^{-7}\ \text{T}^2 - 6.5 \times 10^{-10}\ \text{T}^3$$